Università degli Studi di Napoli "Federico II"

SCUOLA POLITECNICA E DELLE SCIENZE DI BASE

DIPARTIMENTO DI INGEGNERIA INDUSTRIALE

CORSO DI LAUREA IN INGEGNERIA AEROSPAZIALE

CLASSE DELLE LAUREE IN INGEGNERIA INDUSTRIALE (L-9)

Geometric modeling and analysis of stability and control of the Electra Aero aircraft concept

Relatore:
Prof. Danilo Ciliberti

Candidato:
Antonio Niro
Matr. N35003286

ANNO ACCADEMICO 2022 – 2023

Alla mia famiglia, che sempre ha creduto in me.
A chi mi ha insegnato quanto valgo.
E ai miei nonni, so che siete fieri di me.

Abstract

This paper presents a comprehensive study on the geometric modeling and analysis of stability and control of the Electra Aero aircraft concept. The research involves the development of a detailed geometric model of the aircraft, followed by a rigorous analysis of its stability and control characteristics. The geometric modeling is made using JPAD (Java toolchain of Programs for Aircraft Design) software while the analysis of stability and control is made using VSPAERO, one of the tools of OpenVSP suite developed by NASA. OpenVSP can be used to create 3D models of an aircraft and to support different types of analysis of these models. The tool which is used to perform aerodynamics analysis is VSPAERO, a fast, linear vortex lattice solver which integrates actuator disks to perform aero-propulsive analysis. Also, the "Parasite Drag" tool is used to compute the zero-lift drag coefficient. The study aims to provide a deep understanding of the aircraft's aerodynamic behavior and to identify potential areas for design optimization.

Sommario

Questo articolo presenta uno studio completo sulla modellazione geometrica e l'analisi della stabilità e del controllo del concetto di aereo Electra Aero. La ricerca coinvolge lo sviluppo di un dettagliato modello geometrico dell'aereo, seguito da un'analisi rigorosa delle sue caratteristiche di stabilità e controllo. La modellazione geometrica è realizzata utilizzando il software JPAD (Java toolchain of Programs for Aircraft Design) mentre l'analisi della stabilità e del controllo è realizzata utilizzando VSPAERO, uno degli strumenti della suite OpenVSP sviluppata dalla NASA. OpenVSP può essere utilizzato per creare modelli 3D di un aereo e per supportare diversi tipi di analisi di questi modelli. Lo strumento utilizzato per eseguire l'analisi aerodinamica è VSPAERO, un veloce risolutore di vortici lineari che integra dischi attuatori per eseguire un'analisi aero-propulsiva. Inoltre, il tool "Parasite Drag" è stato usato per calcolare il coefficiente di resistenza parassita a portanza nulla. Lo studio mira a fornire una profonda comprensione del comportamento aerodinamico dell'aereo e a identificare potenziali aree per l'ottimizzazione del design.

Sommario

List of figures

1 Introduction

1.1 Objectives

This thesis focuses on the modeling of a particular aircraft which is the Electra eSTOL concept and the subsequent stability and control analysis. The first step is to create a 3D model of the aircraft starting from the 2D render images. Electra Aero confirmed that the dimension of its production 9-seater version will be similar to Cessna Caravan EX [9], while the 2-seater concept is clearly inspired by Tecnam P2006T. The creation of the 3D model is addressed firstly using AutoCAD to scale the dimensions, then entering these geometric information in JPAD it was possible to create the CAD model from which the study started, exporting it appropriately, on the OpenVSP platform. Using the VSPAERO tool and considering the single wing configuration it was possible to obtain the data regarding lift coefficient (C_L), pitching moment coefficient (C_{My}), drag coefficient (C_D) and aerodynamic efficiency (L/D) at different angles of attack (α) and different configuration in terms of flap deflection δ_f and elevator deflection δ_e.

1.2 Layout of the work

Chapter 2: This chapter discusses how *DEP (Distributed Electric Propulsion)* works and its impacts on small airplanes. It also includes the vision behind Electra eSTOL aircraft concept.

Chapter 3: This chapter introduces JPAD and OpenVSP software, with an overview of their main features, focusing on those used to perform the analysis inside the tool of VSPAERO.

Chapter 4: This represent the beginning of the study of the aircraft components and its preliminary geometric modeling, discussing how dimensions are found and how the aircraft concept has been modeled through the software.

Chapter 5: The fifth section of the thesis discusses the data collected through VSPAERO, their organization in graphs and tables with the help of excel sheets, and comparisons between the various curves. It focuses on the effects of various configurations on C_L , C_D, C_{My}, L/D.

Chapter 6: Conclusions chapter.

2 DEP (Distributed Electric Propulsion)

Distributed Electric Propulsion (DEP) is a revolutionary approach to aircraft design, where multiple electric motors and propellers are used to provide thrust. This system distributes propulsion along the wings, allowing for a more efficient lift and significantly reducing fuel consumption. DEP is widely viewed as a promising technology for future aircraft, potentially leading to quieter, more efficient, and environmentally friendly air travel.

2.1 Benefits of DEP

This technology offers several benefits [1]:

- *Enhanced high-lift performance*: DEP allows for the use of smaller wings without compromising low-speed performance. By distributing propellers along the leading edge of the wing, DEP increases the dynamic pressure over the wing at slow speeds, enabling a reduction in wing area and drag at cruise while maintaining low-speed performance. This is particularly useful for light aircraft, which often have oversized wings for their target cruise speeds.
- *Increased overall efficiency*: DEP architectures can yield a net benefit in total efficiency due to synergistic airframe-propulsive coupling. The relatively scale-invariant nature of electric motors enables more distributed propulsion architectures, which can lead to greater aerodynamic efficiency compared to traditional propulsion systems.
- *Reduction in energy consumption*: By retrofitting an existing aircraft with DEP, energy consumption can be significantly reduced compared to the original aircraft. The use of high-lift propellers and wingtip-mounted cruise propellers increases aerodynamic efficiency and reduces propulsive power, resulting in reduced energy consumption at the selected cruise point.
- *Shifting of maximum lift-to-drag ratio*: DEP technology allows for the shifting of the maximum lift-to-drag ratio to higher velocities. This is achieved by enabling the design of a smaller wing with higher maximum lift capability, reducing wing wetted area, and reducing induced drag through the interaction of wingtip-mounted cruise propellers with the wingtip vortex. These factors contribute to an overall increase in lift-to-drag ratio, improving efficiency.

2.2 NASA Sceptor Program

NASA tested DEP using the program “SCEPTOR” which had retrofit an existing internal combustion engine-powered light aircraft (Tecnam P2006T) with two types of DEP: small

"high-lift" propellers distributed along the leading edge of the wing which accelerate the flow over the wing at low speeds, and larger cruise propellers co-located with each wingtip for primary propulsive power.

Figure 1 ***Nasa X57 MAXWELL aircraft (Sceptor program)***

The primary objective of the project is to demonstrate a large reduction in energy consumption compared to a conventionally-powered aircraft of the same size class in cruise. The "stretch" goal is to achieve a fivefold reduction in energy consumption, while the minimum threshold goal is a 3.5x reduction. The lower limit of 3.5x reduction reflects the full benefit of switching propulsion systems, as electric motors can achieve higher efficiency compared to internal combustion engines. The team aimed to meet efficiency multipliers per the project goals, with a minimum 3.5x improvement and a goal of 5.0x reduction in energy consumption. Altitude limitations and the weight of onboard energy storage were also taken into consideration.

The project utilized Tecnam P2006T for retrofit and implemented incremental demonstrations, referred to as "Mods" (up to rev3.3) to help mitigate risk throughout the project. Satisfactory designs were selected based on trade studies that evaluated millions of combinations of wing and propeller designs.

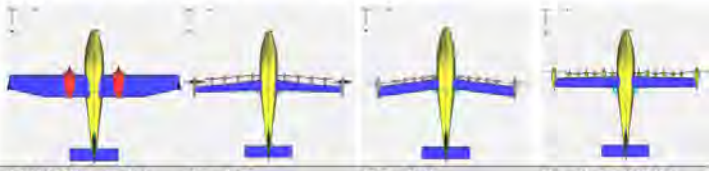

Model	P2006T (stock)	Rev1.2	Rev 2.0	Rev3.3 (PDR)
Span, ft	37.4	33.0	29.2	31.6
Planform area, ft^2	158.9	56.9	57.5	66.7
Wing loading, lbf/ft^2	17.1	52.7	52.2	45.0
Aspect ratio	8.8	19.1	14.8	15.0
Root chord, ft	4.57	2.25	1.97	2.48
Tip chord, ft	2.90	1.20	1.97	1.74
Leading edge sweep, deg	0.0	5.0	7.5	1.9
Cruise propeller diameter, ft	5.84	4.70	5.74	5.00
Cruise propeller speed at cruise, RPM	2250	2470	1500	2250
Number of high-lift propellers	0	8	10	12

Figure 2 ***Different configuration starting from stock aircraft up to REV 3.3***

The SCEPTOR 4.0 configuration, which is currently being developed, includes high-lift propellers along the leading edge of the wing and wingtip-mounted cruise propellers. The high-lift propellers enhance low-speed lift and allow for a reduction in wing area and drag at cruise, while maintaining low-speed performance. The wingtip-mounted propellers enhance aerodynamic efficiency and reduce propulsive power by interacting with the wingtip vortex.

The 4.0 configuration has been developed with minor changes from the previous version, Rev3.3. The major specifications for both versions are identical. The changes include a larger wingtip cruise nacelle to accommodate the latest motor and additional components, as well as a translation of the propeller disc to reduce structural issues. There have also been modifications to improve motor cooling and the selection of a commercially available propeller. The high-lift propeller discs have a staggered arrangement for safety and folding capability. The high-lift nacelles are placed on pylons under the wing, and the exact offset and length of pylons are still being determined. Using pylons instead of integrated nacelles allows for wing design flexibility and reduces aerodynamic impact.

The goal of the project is to significantly reduce the energy consumption of the aircraft at the selected cruise point compared to the original aircraft. The efficiency improvement goal is approximately 4.8x better than the stock aircraft at a selected cruise point of 150 knots true airspeed and 8,000 feet altitude [3].

Another interesting test is the *LEAPTech* (Leading Edge Asynchronous Propeller Technology) /*HEIST* Experiments Test. The intended purpose of the *LEAPTech/HEIST* experiment was to test the Hybrid-Electric Integrated Systems Testbed (HEIST) in order to demonstrate large improvements in efficiency, emissions, safety, and operating costs for general aviation sized aircraft with Distributed Electric Propulsion (DEP). The experiment

aimed to show high wing loading, which would improve ride quality and takeoff/landing characteristics. The ultimate goal was to obtain data and verify the performance of the blown wing, primarily with regards to lift.

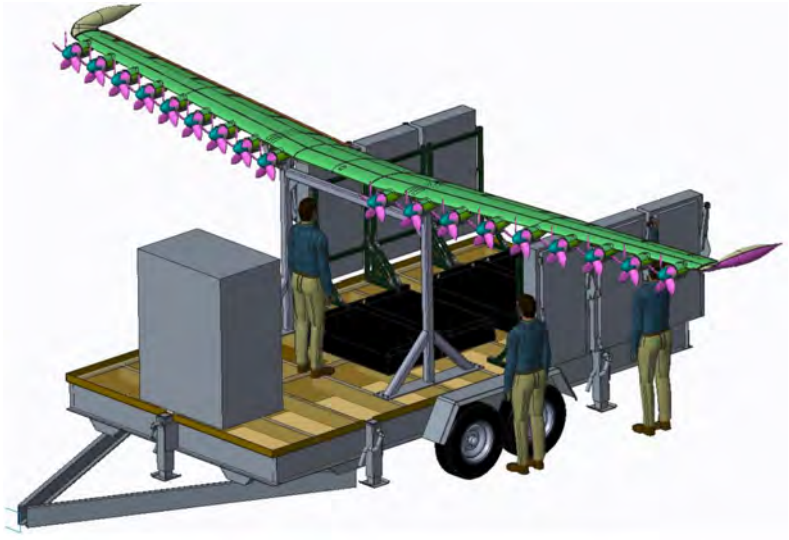

Figure 3 ***HEIST test. Wing with DEP tested at nasa***

The wing on the HEIST experimental setup was designed with several specifications to streamline construction and deliver useful data and analysis. The center section of the wing is straight, while the primary wing sections have a constant linear taper, sweep, and twist. The wing incorporates eighteen brushless electric Joby JM1 motors, which are evenly spaced spanwise and mounted in nacelles along the wing leading edge. The wing also features Fowler flaps that can be manually set at 0, 10, 20, 30, or 40 degrees. The wing angle of attack can be adjusted manually by adjusting the pin position on the supporting structure connections/load cell assembly. The test article wing underwent testing in both a blown and unblown configuration. The blown configuration refers to the wing with propellers, no spinners, and the motor on, while the unblown configuration refers to the wing without propellers, no spinners, and the motor off [4].

2.3 Electra Aero eSTOL concept

Given the benefits of DEP (Distributed Electric Propulsion) shown from theoretical and practical point by the NASA SCEPTOR program, it is clear that a player is needed to propose a solution with such advantages in the marketplace. The main player on the market is Electra Aero, a startup founded in 2020 in the United States of America that aims to create an electric ultra short take-off and landing aircraft to cover short distance routes and that will carry 9 people onboard for around 400 NM (Nautical Miles). The designed cruise speed will be at 175 knots

(324 km/h) and it will only need 300 ft (91,44 m) to take-off thanks to its blown lift technology, a special aerodynamic technique that multiplies lift.

Figure 4 ***Electra's eSTOL 3D render. available at www.electra.aereo***

The idea has been highly appreciated and in fact the company has received several rounds of investment, plus in winter 2021 Lockheed Martin joins Electra as strategic investor [7].

At the time of writing this thesis, there is no model on the market, only renderings on which dimensions are derived. The dimensions taken from the concept will be discussed in chapter 4.

3 Software

3.1 JPAD

The next step after finding the scaled dimensions of the 3D render of the eSTOL designed by Electra using AutoCAD is to import the significant dimensions into JPAD, which stands for "Java toolchain of Programs for Aircraft Design". JPAD is conceived as an ecosystem of interconnected modules aimed at providing a reliable, fast and efficient tool to support the design, the analysis and the optimization of transport aircraft.

JPAD presents itself with the following interface, divided into two parts: on the left side is the "components" section where you can enter all the appropriate input values, divided into components. In fact, it is possible in the "manage components" section to add or remove the desired components present in the aircraft we are modeling. Once added or removed, it will be enough to press the "update" button to have the requested changes executed. With the JPAD tool, you can work on the following components:

- Wings on which it is possible to add flaps, slats, ailerons, or winglets
- Fuselage and cabin, working on all geometric parameters as also number of passengers, seats, cabin crew
- Tail plane
- Nacelles and powerplant
- Landing gear.

The right section is instead dedicated to the real-time view of the aircraft we are modeling using a CAD, with the possibility of selecting the preferred view. There is also a part at the bottom that gives us the possibility to view information related to the CAD and the geometry of the aircraft.

3.2 OpenVSP

OpenVSP, short for Open Vehicle Sketch Pad, is a free, open-source tool for developing parametric aircraft geometry. Initially created by NASA under the NOSA license in January 2012, it allows users to design three-dimensional aircraft models and aids in the engineering examination of these models, with different tools to perform various analysis.

You can visit the OpenVSP website using the following link: www.openvsp.org

Upon launching OpenVSP, once a .vsp3 file is opened, you will see a working window and a "Geometry Browser". It displays all the individual components of your model, allowing the user to modify the parameters of the selected component. OpenVSP provides multiple geometries common to aircraft modeling that can be modified and assembled into an aircraft model, e.g., wing, pod, fuselage, propeller.

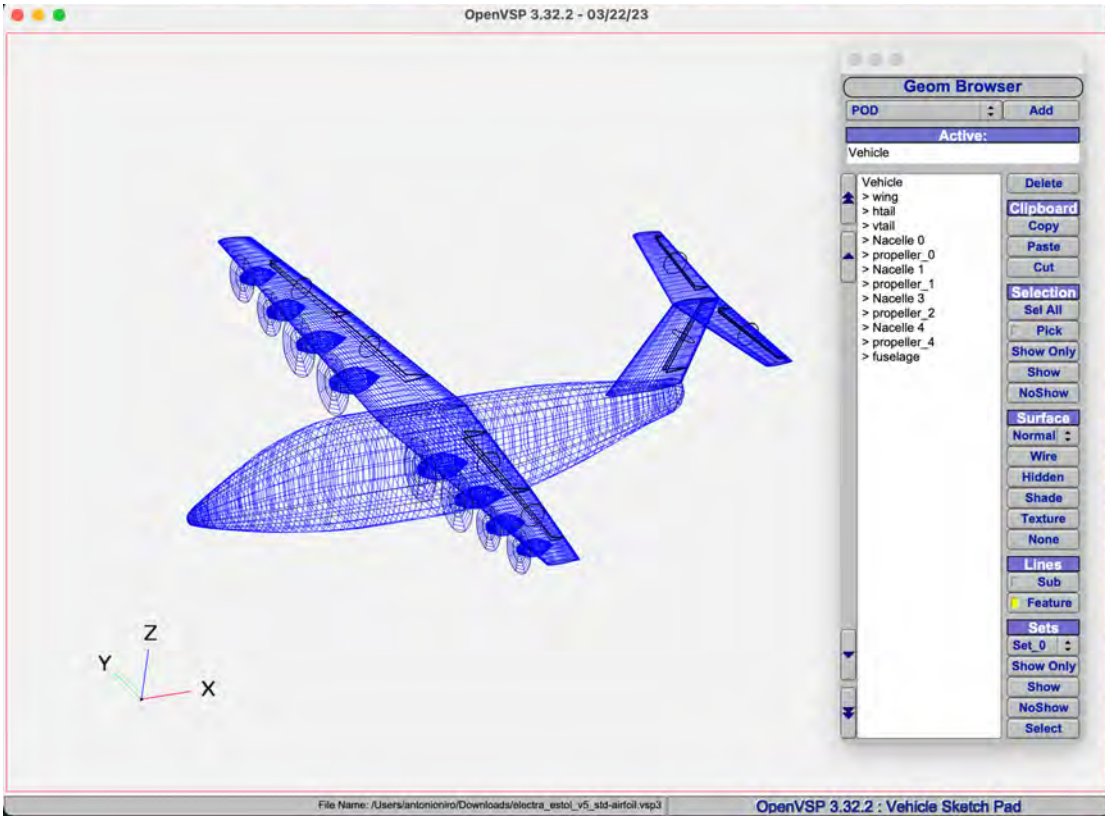

Figure 5 ***Electra's concept visualized in OpenVSP viewer main page***

3.3 VSPAERO

VSPAERO is one of the different tools integrated in OpenVSP. It is a linear vortex lattice solver that analyzes closed surfaces to provide an aerodynamic analysis based on a given set of flight conditions (e.g. cruise speed, angle of attack α angle of sideslip β and control surfaces deflections).

The degenerate geometry file (.deg) is required to perform the analysis. Each panel generated in the OpenVSP degenerate geometry file has discrete vortices applied to it. These vortices are then assessed across the entire surface, resulting in a pressure distribution. This distribution provides force data, which can be utilized to calculate lift, drag, slip, and the forces and moments in the x, y, and z directions.

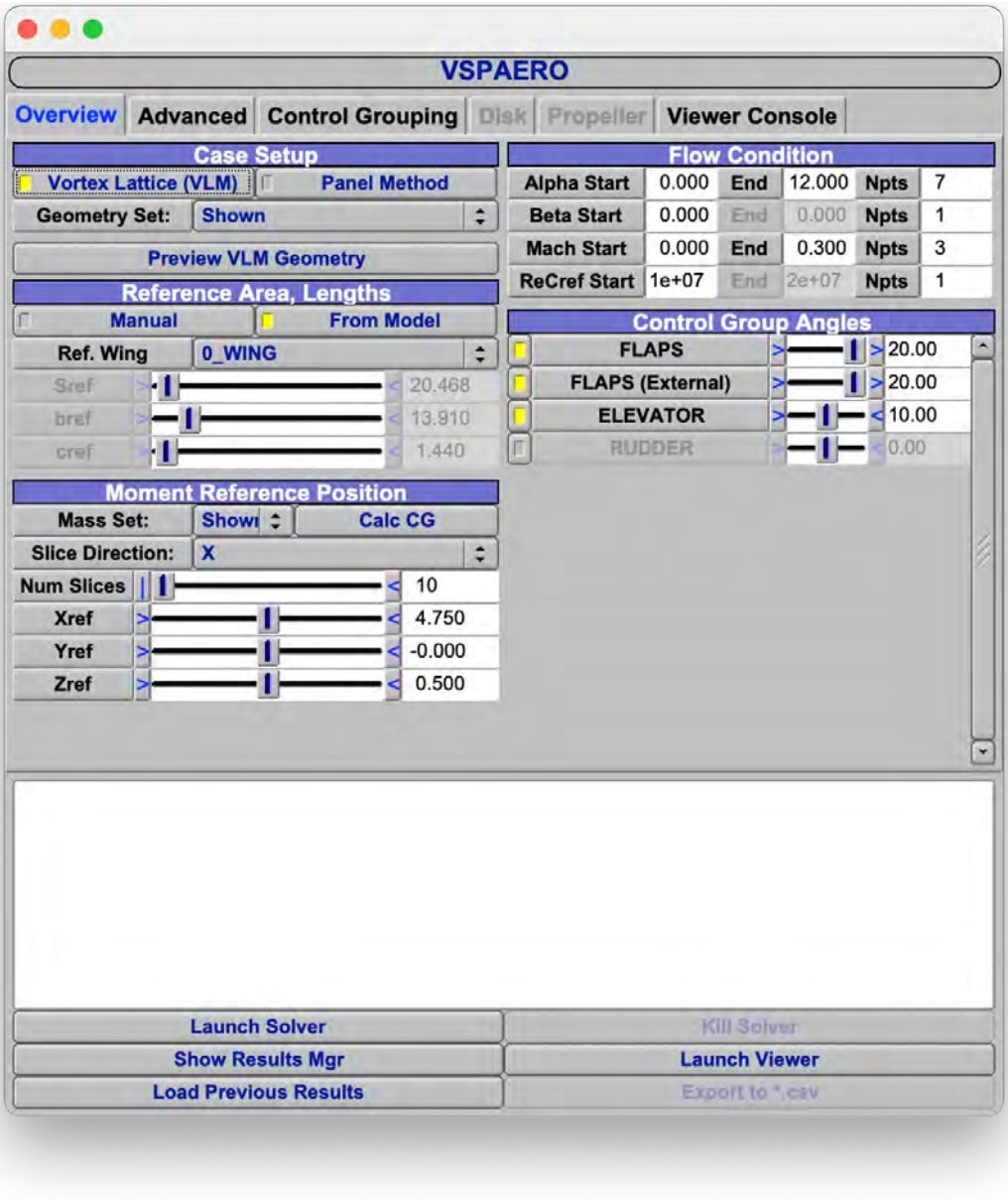

Figure 6 ***VSPAERO Overview panel.***

VSPAERO "Control Grouping" section allows the definition of groups of control surfaces.

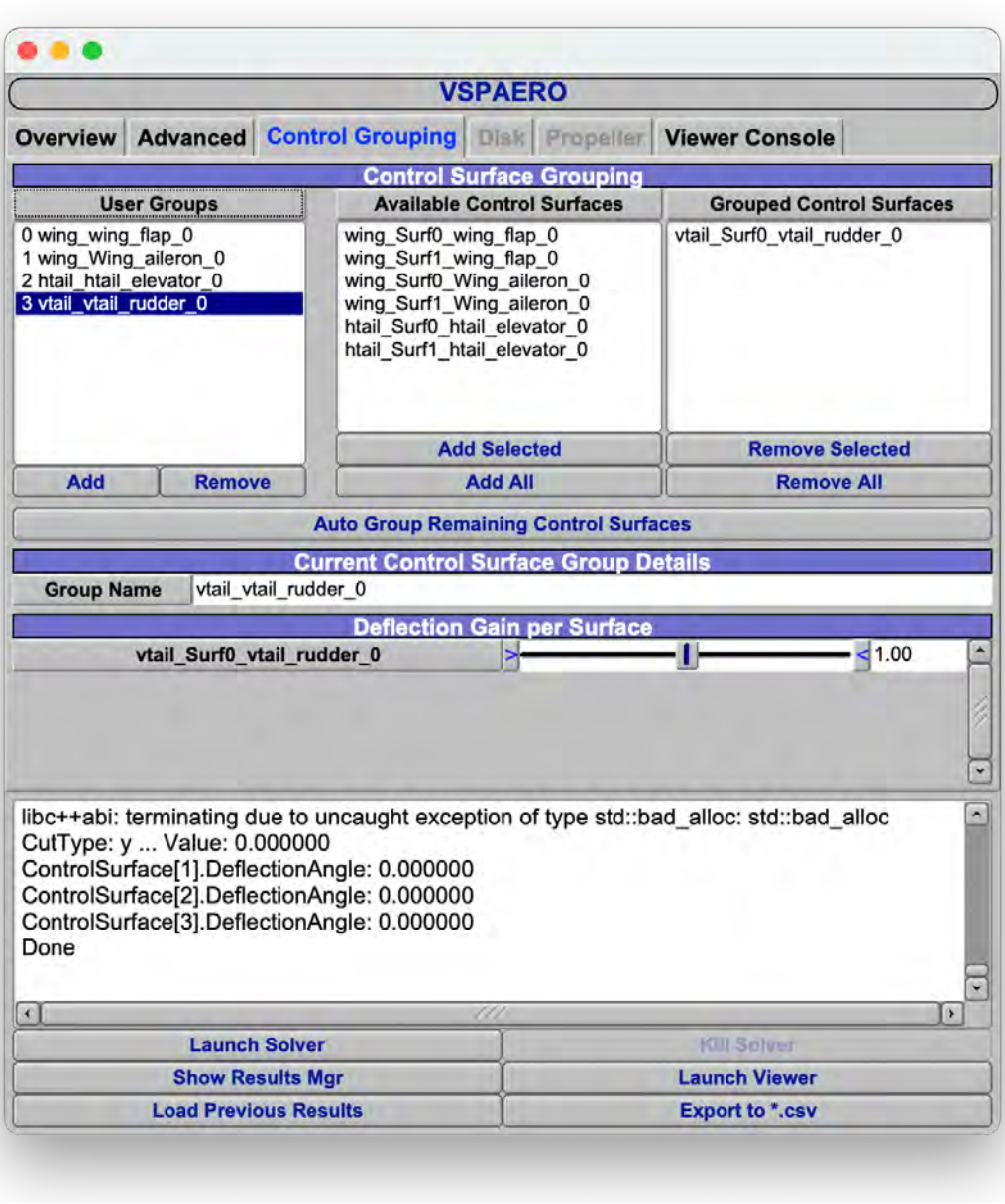

Figure 7 ***VSPAERO Control Grouping Section***

It is crucial to understand that unless a geometry set is specified, DegenGeom will pin down all components in a model. You can generate degenerate geometry files for your chosen components from OpenVSP, either by selecting DegenGeom from the Analysis menu or by clicking Launch Solver in the VSPAERO GUI. The file will be recognized as *modelname_DegenGeom.vspaero* if you're using the vortex lattice method and *modelname.vspaero* for the panel method.

The simplest approach to create a file for a new model is to open VSPAERO, select the Overview tab, and use the provided sliders and inputs to define a Setup file. After setting up the flow conditions to be analyzed, the Launch Solver button will automatically produce the Setup file and initiate VSPAERO with the VLM setup.

Upon viewing the *.vspaero* file, you'll notice that most of the values have been filled in. This includes:

- The *History* file, which holds integrated values calculated by VSPAERO for each iteration, including the lift coefficient, induced drag, and force and moment coefficients.
- The *LOD* file, which offers a spanwise depiction of the local lift, drag, and side force coefficients. This file is beneficial for final vehicle plots.
- The *ADB* file, which includes ADB-related information.
- The *Stability File* (STAB) holds the output of the stability analysis, which can be produced by selecting one of the following sets in the Advanced tab: Stability, P Analysis, Q Analysis, R Analysis.
- The *FEM* file, which records the aerodynamic forces and moments for each spanwise station in a wing section.

4 Geometry and study of the Electra aircraft concept

4.1 Electra eSTOL concept geometry

Electra eSTOL (ultra short take-off and landing) concept (2-seater) uses similar design as Tecnam P2006T, while the production version (9-seater) will have similar dimension to Cessna Caravan which also carries 9 people onboard.

The dimensions of the concept were found by scaling the front and side view of the render with the length of the Cessna Caravan (https://cessna.txtav.com/en/turboprop/caravan#_model-specs) on AutoCAD and then imported in JPAD modeler. The starting dimension is the length of the aircraft of 37 ft 7 inches (equal to 11.45 meters).

Figure 8 ***Electra's eSTOL concept frontal view***

Figure 9 ***Electra's eSTOL concept lateral view***

Wing Geometry

The first and main element to study of our model is the wing, characterized by a wingspan of 13.91 m and a wing area of 20.468 m^2 which leads to and aspect ratio AR = 9.427. Pay attention to the fact that parameters in OpenVSP do not explicitly show units, so it is the user's task to enter and use data that are dimensionally consistent.

The innermost chord has a size of 2.107 m while the wingtip is 0.77 m. Therefore, a taper ratio can be defined as: $\lambda = \frac{c_{tip}}{c_{root}}$ which is equal to 0.3654. NACA 2215 is the chosen airfoil profile. Dihedral angle is 4°.

Fuselage

As any other geometric component, the fuselage has its own geometric modeling window. With the possibility to place the render image behind the 3D model, it was possible to recreate the right curvature of the fuselage by changing the parameter Z. Fuselage is composed by three parts: the nose trunk which has 3.51m that includes 0.751 m of nose cap; cylindrical trunk is 2.503 m long and tail trunk is 5.437 m of which 0.491m is occupied by the tail cap. The maximum width is 1.94 m and the maximum height of the cabin is 2.107 m.

Tail Plane

The horizontal tail can also be modeled geometrically. Similar to the wing, the basic geometric parameters should be entered in the design window. For the horizontal tail plane, the NACA 2212 is the designed profile, while for the vertical tail plane a symmetric airfoil is chosen, more specifically a NACA 0012. Horizontal plane has a root chord of 1.105 m and tip chord of 0.642 m. The span of horizontal tail plane is of about 5.60 m.

Control surfaces

There are two flaps for each of the two wings, as well as an elevator on the horizontal tailplane and a rudder on the vertical tailplane.

Landing gears and winglets are not considered in the 3D model used to perform the stability and propulsive analysis.

4.2 Geometry modeling in OpenVSP

These geometric data formed the basis upon which the aircraft was designed and created on JPAD. Once this data has been exported, it becomes possible to visualize the aircraft in a different environment – OpenVSP. This software allows for a more in-depth exploration of the aircraft's structure.

In addition to the basic structure of the aircraft, OpenVSP also presents the various control surfaces of the aircraft. These are key components that contribute to the aircraft's maneuverability and stability. The integration of these control surfaces into the visual model enables users to perform in-depth stability analyses. They can simulate and observe the aircraft's performance under a variety of deflection conditions, gaining valuable insights into its behavior under different operating scenarios. Landing gear has been neglected in the following model.

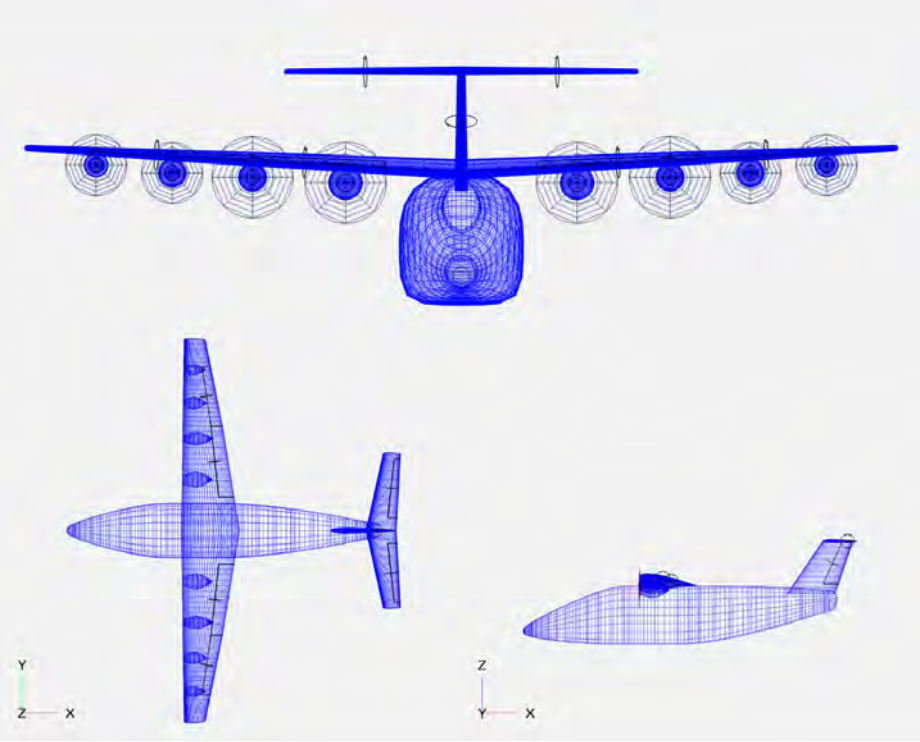

Figure 10 ***Aircraft visualized in OpenVSP (view comparison).***

The first and bigger element of Electra Concept is the fuselage. The fuselage is divided in three main parts: nose trunk, cylindrical trunk and tail trunk. In JPAD is also necessary to model

the nose cap and tail cap. On OpenVSP the fuselage is divided in 37 cross sections. Figure below shows the form of fuselage and the parameters used for some sections to model the fuselage.

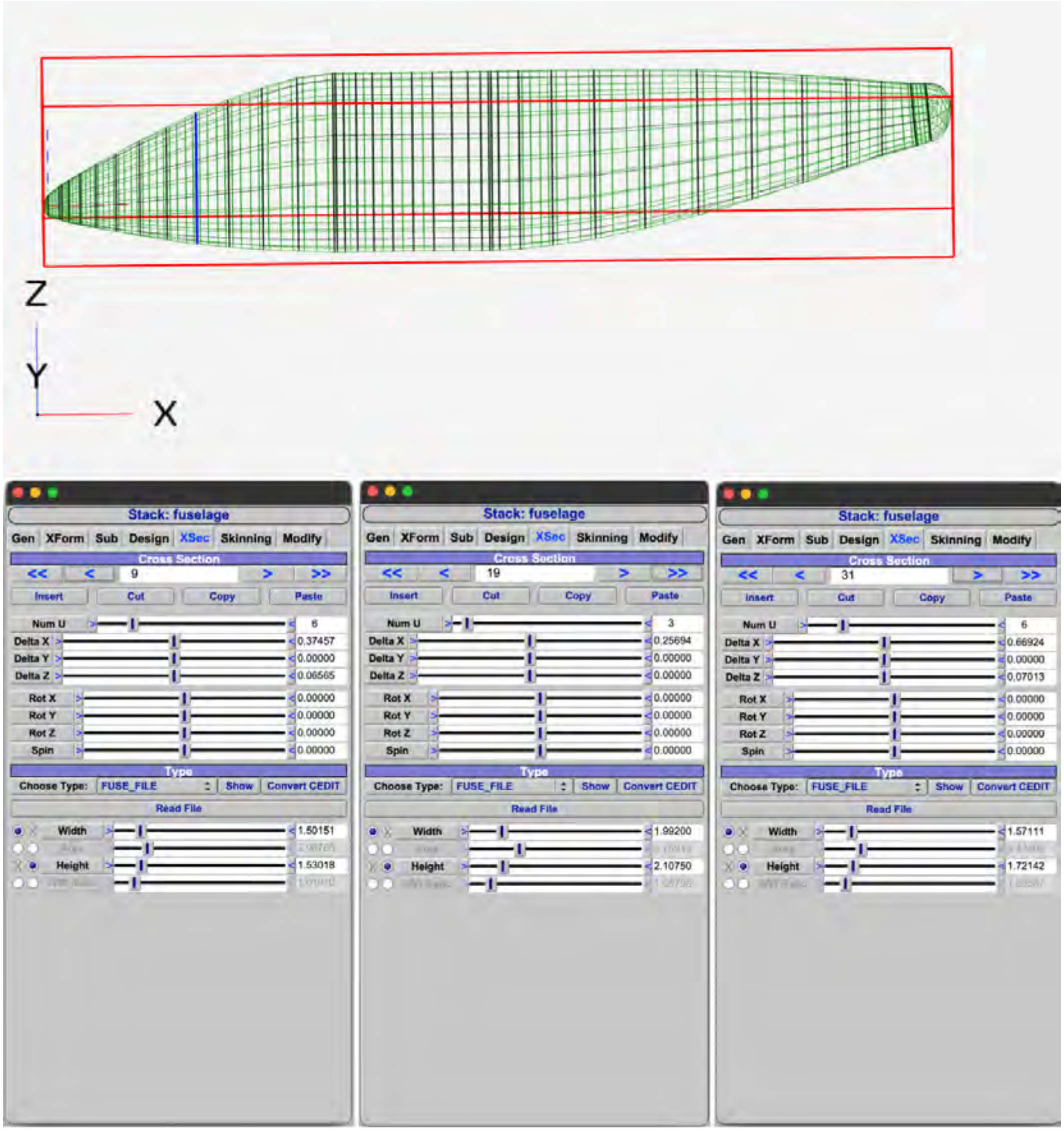

Figure 11 ***Figure Gen and XSec panels for fuselage sections.***

For the wing the airfoil in consideration is a NACA 2215, based on NACA 0015 with 2% camber. The wing is composed by two different panels with two different taper ratio. There are four movable surfaces, two per panel. Horizontal plane has instead NACA 2212 airfoil profile. Figures below shows the geometric parameters for wing and for horizontal plane.

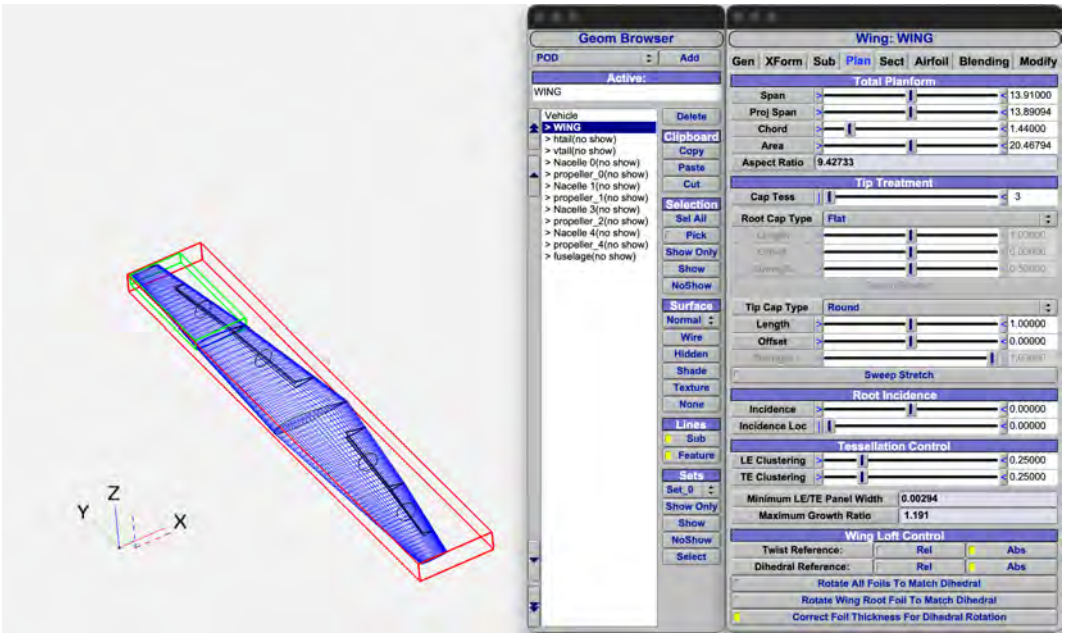

Figure 12 ***Wing 3D. Plan panel in VSPAERO.***

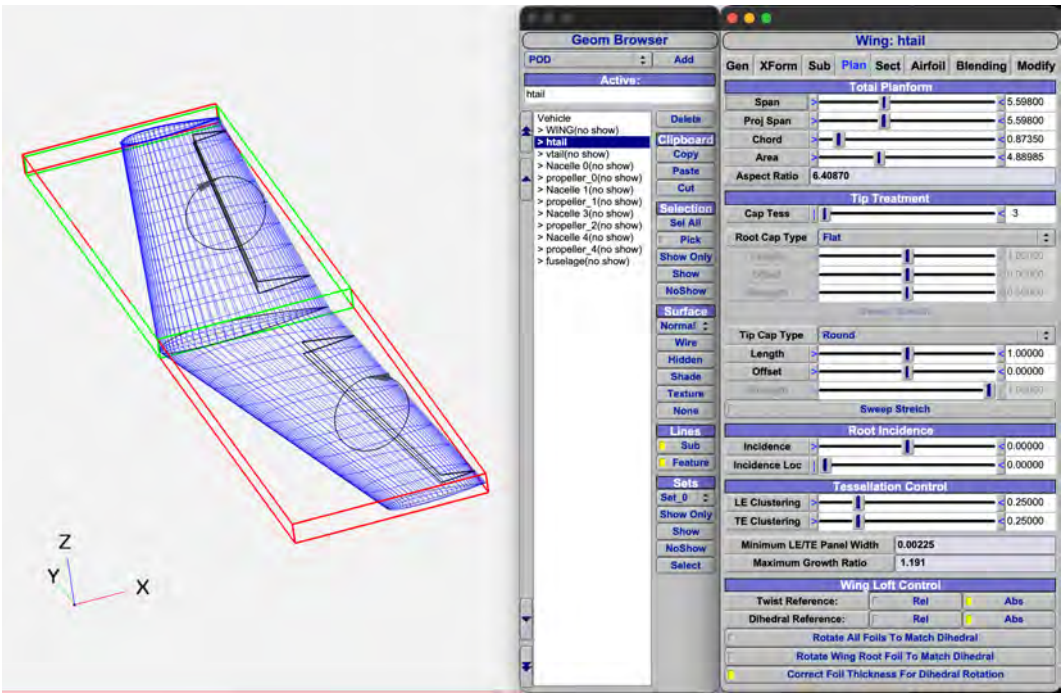

Figure 13 ***Horizontal Tail Panel 3D. Plan panel in VSPAERO.***

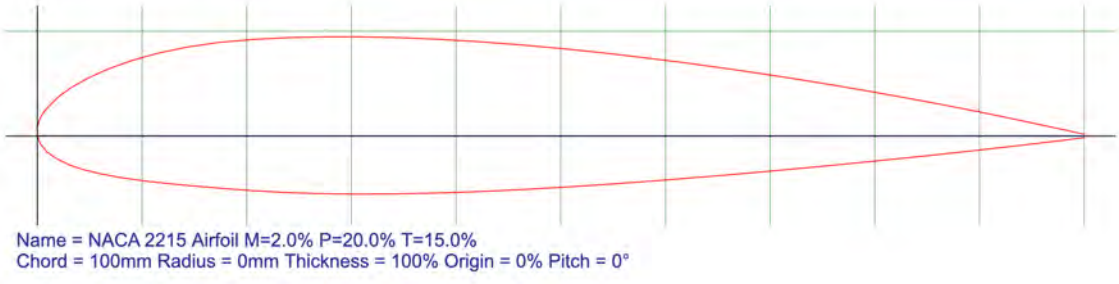

Figure 14 ***NACA 2215 profile used for wing, plot from airfoiltools.com.***

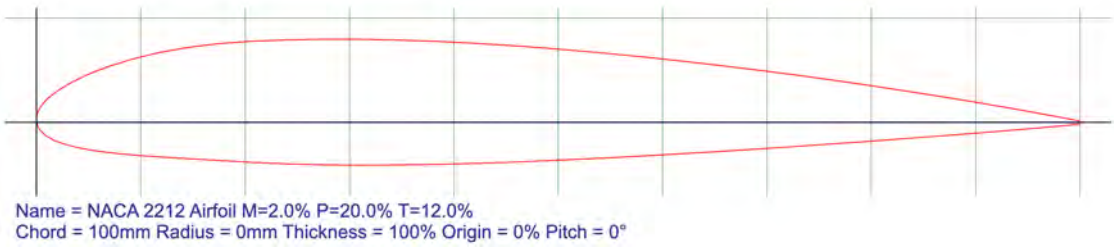

Figure 15 ***NACA 2212 profile used for wing, plot from airfoiltools.com.***

The tail of the concept analyzed in this paper has a T shape, on which horizontal plane is mounted on top of the vertical plane. Vertical panel has a symmetrical airfoil, the NACA 0012. Geometric details are: span of 1.902 m, chord of 1.431 m and area of 2.72 square meters which leads to AR of 1.329. Geometric parameters and design are shown below.

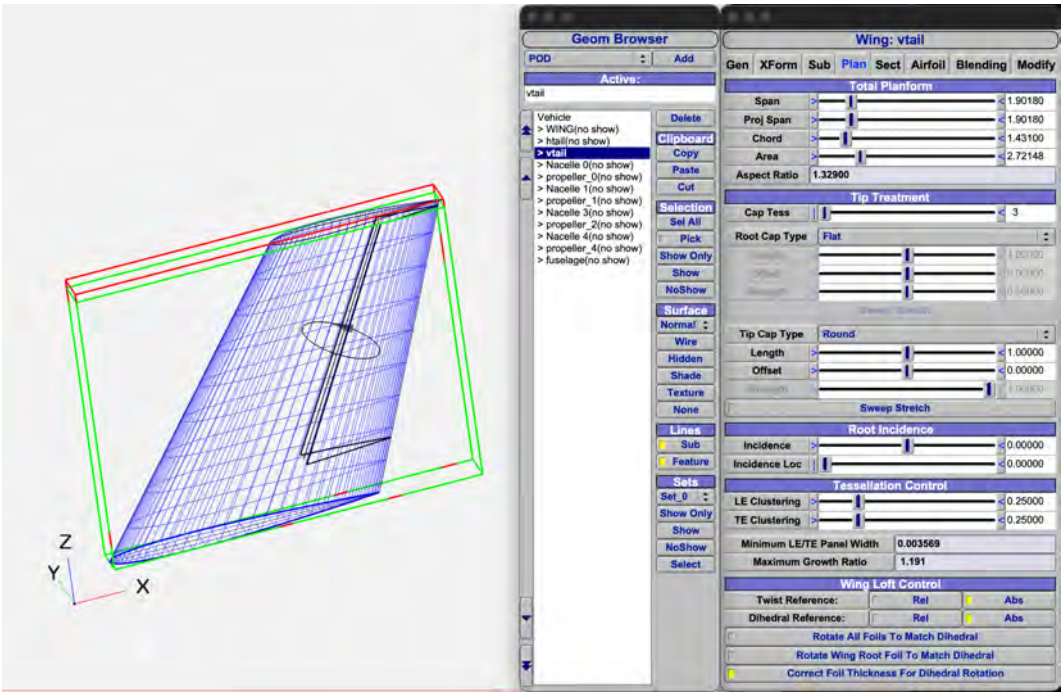

Figure 16 ***Vertical Tail Panel 3D. Plan panel in VSPAERO***

Speaking of control surfaces present, they are visible and can be grouped in the “Control Grouping” panel of the VSPAERO tool, which will then allow us to perform accurate analyses at different deflections. In particular, we have: flaps (internal and external), stabilizer, and rudder.

Figure 17 ***Sub panel for: wing, horizontal tail and vertical tail***

As discussed in section 2 concerning the DEP, several thrusters are mounted on the wing, specifically eight thrusters, mounted under the wing, four on the left and four on the right.

The thrusters are modeled as actuator disks and for each thruster there is a propeller and a nacelle. They come in two different sizes: the two inner thrusters are larger and have a propeller diameter of 1.302 m while the outer ones have a smaller diameter of 0.98 m.

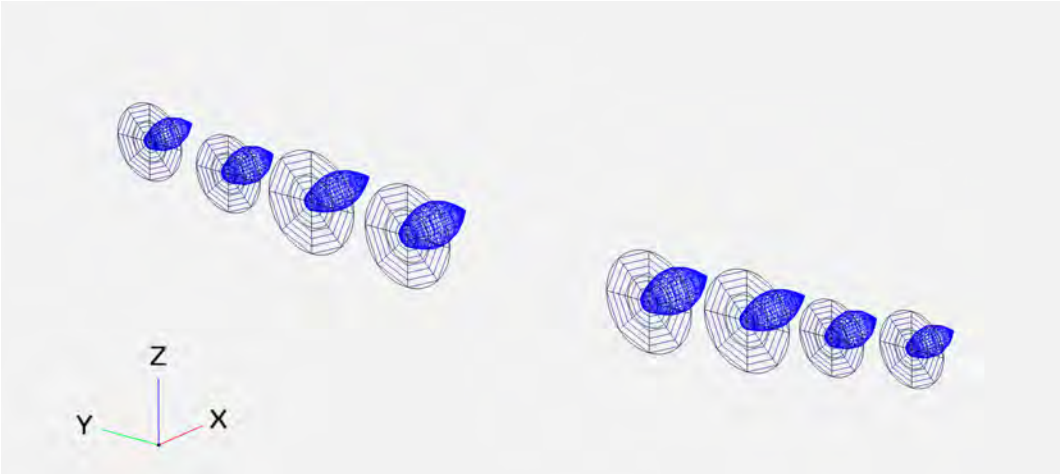

Figure 18 ***Nacelle and propeller 3D design.***

5 Results and discussions

Every aerodynamic and stability analysis was performed using VSPAEREO tool with VLM (Vortex Lattice Method) as case setup. References area and lengths were calculated from model while for Moment Reference Position the CG was set in two different positions. Firstly at $X_{CG} = 4.75$, $Y_{CG} = 0$, $Z_{CG} = 0.5$ and 10 (default) was used as number of slices, and in a second instance the center of gravity was set at $X_{CG} = 3.7, Y_{CG} = 0, Z_{CG} = 0.5$.

The flow conditions were modified to have of values of angle of attack (α) ranging from 0° up to 12°. Sideslip angle (β) is assumed constant as no lateral analysis is performed. These parameters are settable in "Flow condition" panel on the right upper corner in VSPAERO overview, as shown in figure 6.

Both flap deflection and elevator deflection are modified using "Control Group Angles" panel. Positive δ_e values represents the elevator deflecting downward while negative values of δ_e indicate the elevator deflecting upward.

Figure 19 ***Control Group Angles. Flaps, elevator and rudder deflection can be set.***

In regard to flap deflection (δ_f), the analysis is performed at 0°, 10°, 20°, 30°, while elevator is deflected (δ_e) from -10° up to 30°. The results of the analysis are shown in the following section and tables.

An analysis of optimal CG position is performed using the δ_f=0° and δ_f=20° configuration.

For each configuration stability derivatives ($C_{M\alpha}$), residual moment coefficient (C_{M0}) and power control derivatives ($C_{M\delta}$) are calculated. $C_{M\alpha}$ is the slope of the linear regression of C_{My} in function of angle of attack (α) and is computed using excel function "slope". C_{M0} is the intersection of the linear regression of the same curve and is computed using excel function "intersect". $C_{M\delta}$ is the power control derivative of the elevator and it computed using the following formula:

$$C_{M_\delta} = \frac{C_{M_0}(\delta) - C_{M_0}(\delta = 0\,\mathrm{deg})}{\delta}$$

The effects of DEP on aerodynamics and stability were discussed in Section 5.4. In particular, there are three configurations studied: cruise (*prop-on cruise*), climb (*prop-on climb*), and take-off (*prop-on take-off*) and are compared with the *prop-off* case. The propulsive analyses are done with clean wing configuration, so $\delta_f = 0°$, $\delta_e = 0°$. Propellers are treated as actuator disks, and the coefficients needed to carry out the analyses are C_T (thrust coefficient), C_P (shaft power coeffcient), and the calculation and estimation of the thrust and power needed or required under different flight conditions is then required. The formulas and assumptions used are discussed in the respective section.

5.1 Analysis of Electra's eSTOL concept configuration

In the following analysis the T-tail configuration will be called "H.H.T.P." (High Horizontal Tail Plane).

5.1.1 Flaps deflection effects on C_L, C_D, C_M, L/D at Mach=0

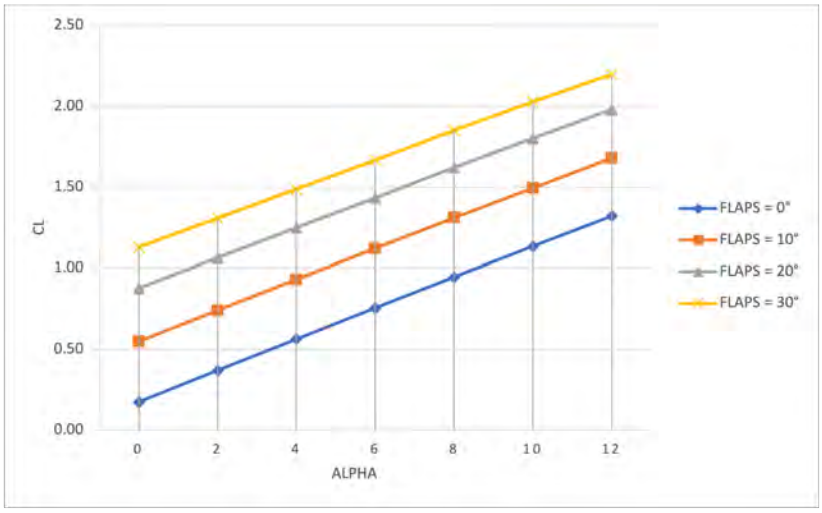

Figure 20 ***Flap deflection effects on C_L for H.H.T.P configuration with X_{CG} = 4.75m***

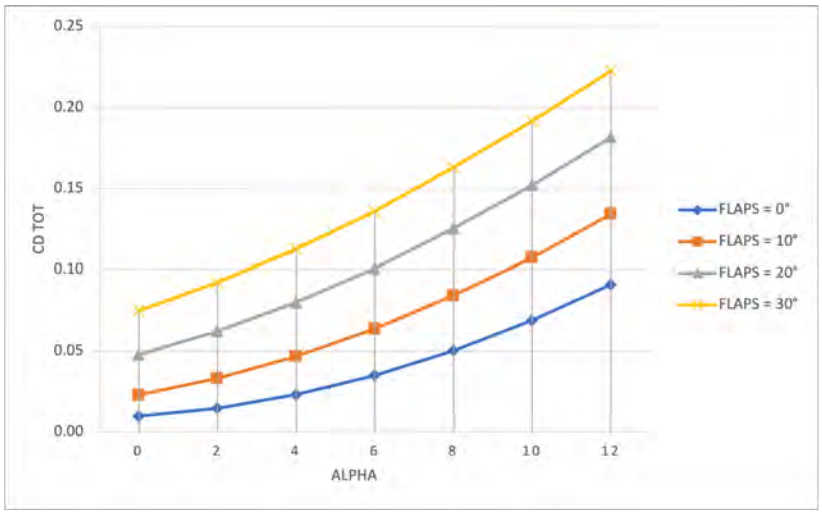

Figure 21 ***Flap deflection effects on C_D for H.H.T.P configuration with X_{CG} = 4.75m***

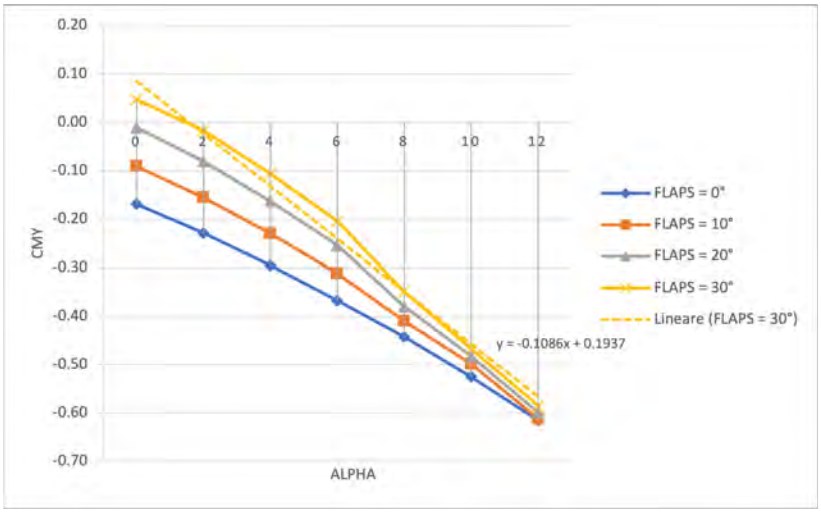

Figure 22 ***Flap deflection effects on C_{My} for H.H.T.P configuration with X_{CG} = 4.75m***

To note that in this particular configuration, the C_{My} curve for more deflected flap has greater value with respect to less deflected flaps.

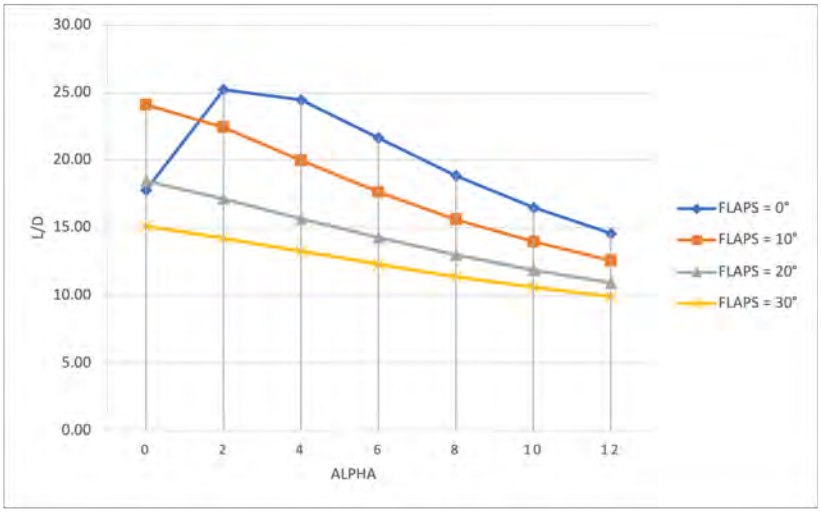

Figure 23 ***Flap deflection effects on L/D for H.H.T.P configuration with X_{CG} = 4.75m***

5.1.2 Elevator deflection effects on C_L, C_D, C_M, L/D at Mach=0 in clean wing configuration

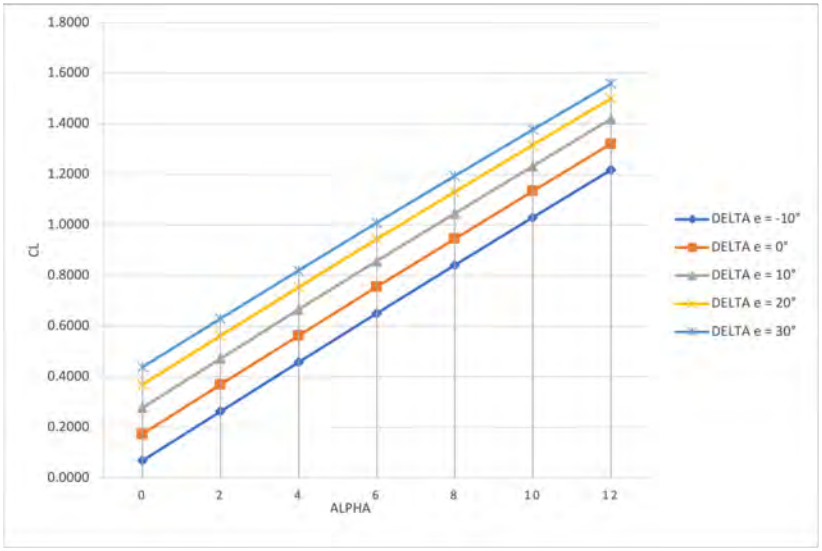

Figure 24 ***Elevator effects on C_L for H.H.T.P configuration with X_{CG} = 4.75m***

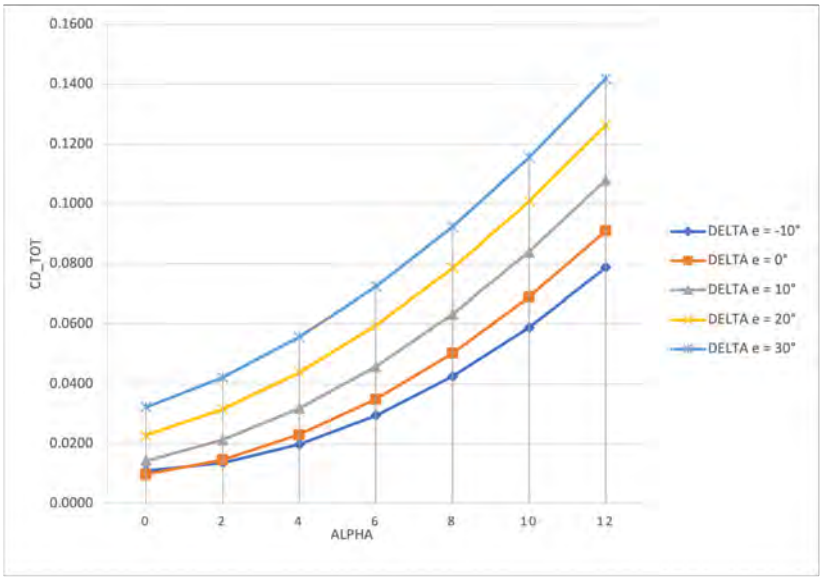

Figure 25 ***Elevator effects on C_D for H.H.T.P configuration with X_{CG} = 4.75m***

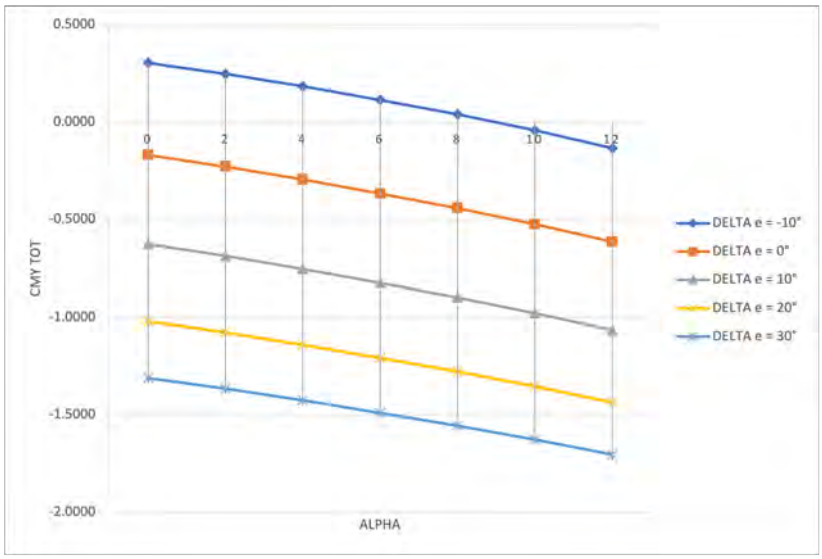

Figure 26 ***Elevator effects on C_{My} for H.H.T.P configuration with X_{CG} = 4.75m***

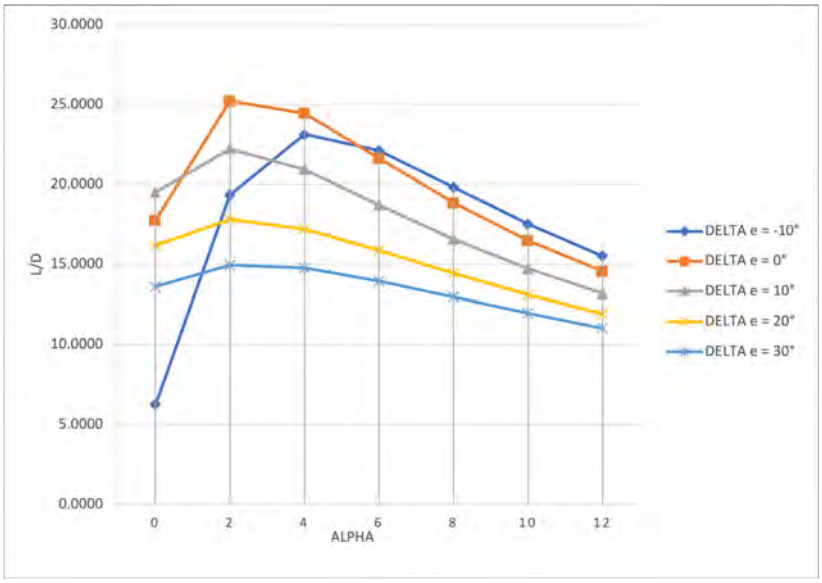

Figure 27 ***Elevator effects on L/D for H.H.T.P configuration with X_{CG} = 4.75m***

5.1.3 Elevator and flaps combined deflection effects on C_L, C_D, C_M, L/D at Mach = 0

5.1.4 Derivatives

Table 1 shows the values for stability derivatives ($C_{M\alpha}$) and elevator control derivatives ($C_{M\delta}$) for this configuration.

δf	*CMα*	*CM0*
0	-0.037	-0.155
10	-0.043	-0.070
20	-0.050	0.017
30	-0.054	0.085

δe	*CMy_tot*	*CMα*	*CM0*	*CMδ*
-10	0.303	-0.036	0.319	-0.047
0	-0.169	-0.037	-0.155	n.a.
10	-0.628	-0.036	-0.615	-0.046
20	-1.020	-0.035	-1.009	-0.043
30	-1.311	-0.033	-1.301	-0.038

Table 1 ***Stability and control derivatives (in deg^{-1}) for L.H.T.P. configuration with X_{CG} = 4.75m***

5.1.5 Results and possible solutions

The analysis performed on Electra eSTOL concept as shown in *Figure 10* shows consistent data and curves on elevator deflection effects in clean wing configuration on every coefficient while analysis of the effect of flap deflection shows inconsistent data for the aerodynamic moment coefficient (C_{My}) since, theoretically, C_{My} should be more negative with increasing flap deflection (i.e., the curve of C_{My} as a function of α with δ_f at 30° should be below the curve of C_{My} with δ_f at 0°).

The position of an aft horizontal tail with respect to the wing is critical. It is possible that the horizonal panel of this T-tail configuration enters the wing wake, causing an instability on the aircraft. Below it is shown a figure took from "Raymer: Aircraft design" [6] at page 71 which shows the optimal positioning of the tail plane with respect to the wing.

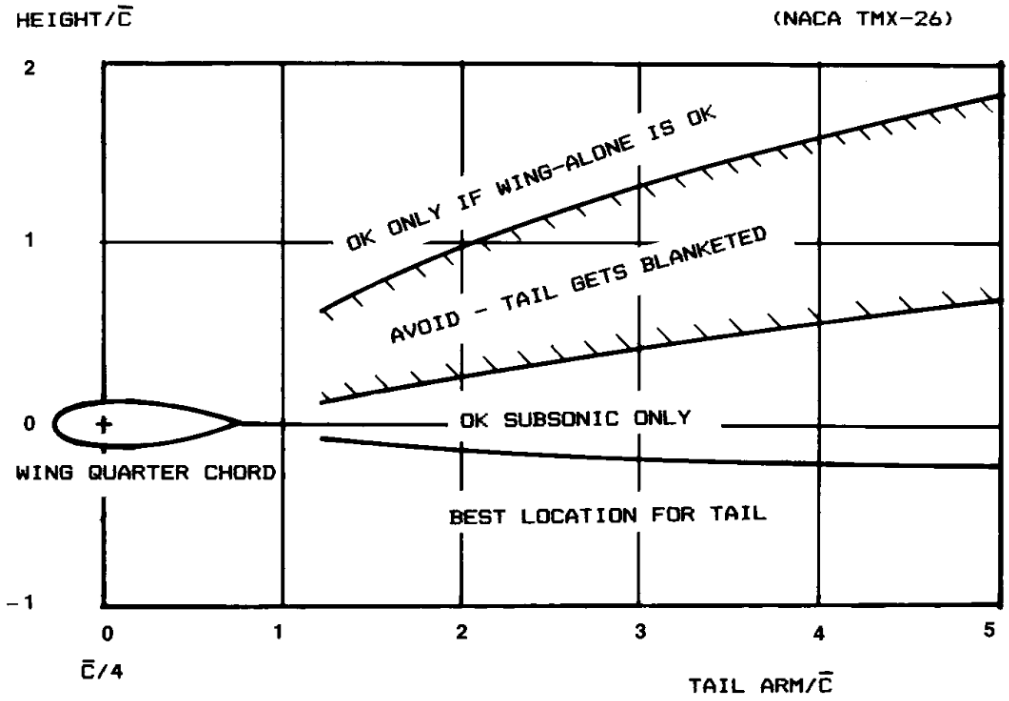

Figure 28 ***Optimal positioning of tail plane with regards to wing. Ref. to "Raymer. Aircraft Design" [6]***

To solve the problem of inconsistent curve of C_{My} a design operation is performed, lowering the horizontal tail plane. This configuration will be called "L.H.T.P" (Low Horizontal Tail Plane).

5.2 Design and Analysis of Electra eSTOL concept with low horizontal tail plane configuration

Using the geometry modeler of OpenVSP the horizontal panel of the tail is moved in the suggested optimal zone. More specifically the panel is moved from $Z = 3.248$m to $Z = 1.075$m, with the same X and Y.

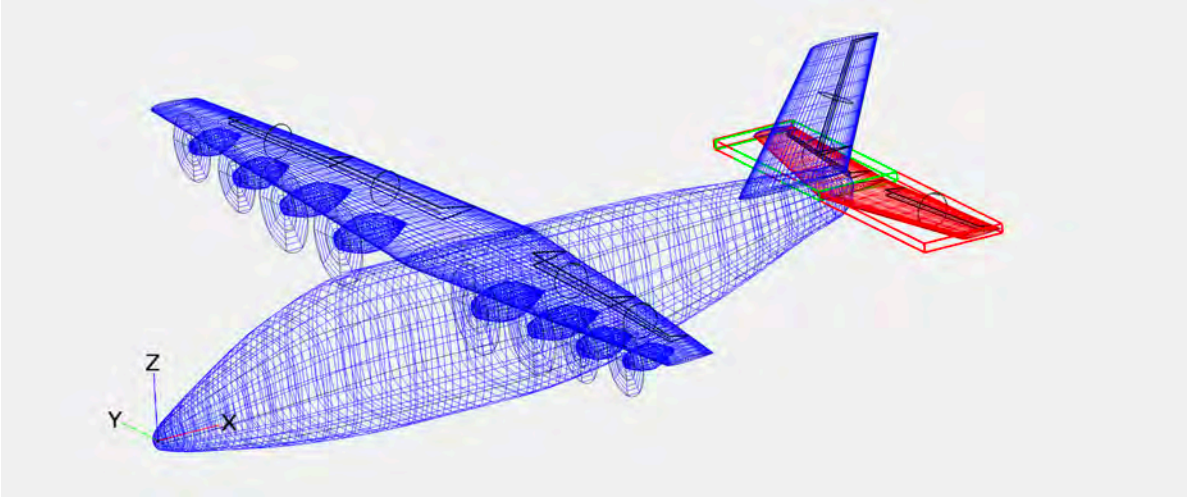

Figure 29 ***L.H.T.P. 3D configuration in OpenVSP. Horizontal plane highlighted in red.***

Stability and control derivatives are calculated with respect to δ_f ranging from 0° up to 30° and δ_e ranging from -10° up to 30°.

5.2.1 Flaps deflection effects on C_L, C_D, C_M, L/D at Mach=0

Graphs below shows the effects of δ_f, on each of the parameter.

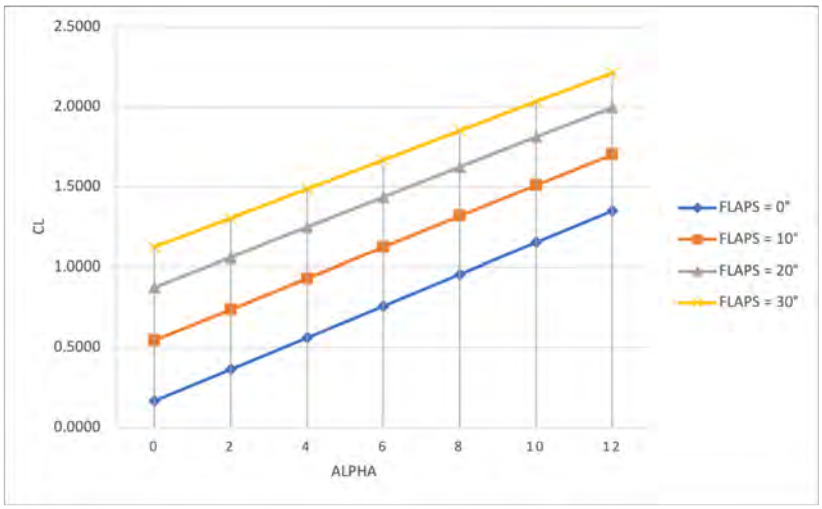

Figure 30 ***C_L with flap deflection for H.H.T.P. with X_{CG} = 4.75m***

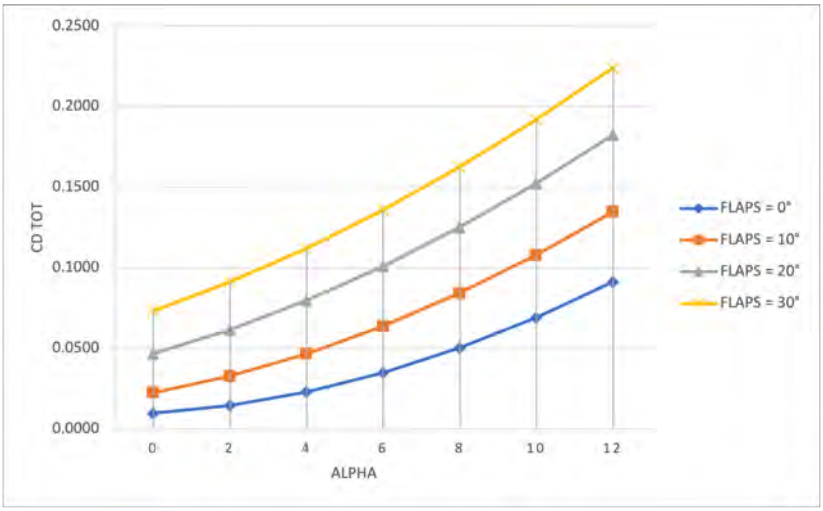

Figure 31 ***C_D with flap deflection for H.H.T.P. with X_{CG} = 4.75m***

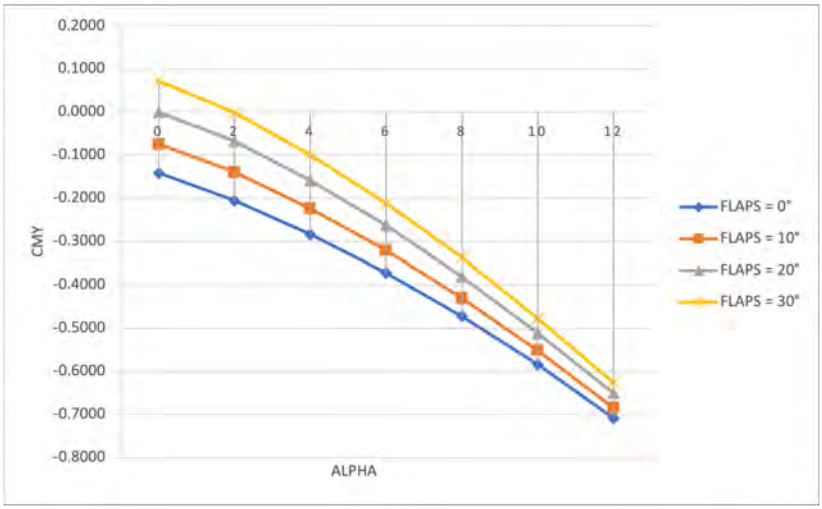

Figure 32 ***C_{My} with flap deflection for H.H.T.P. with X_{CG} = 4.75m***

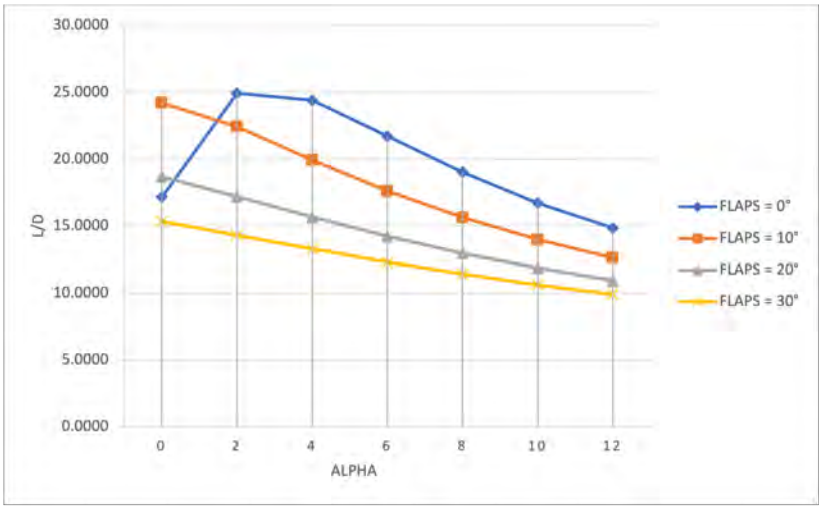

Figure 33 ***L\D with flap deflection for H.H.T.P. with X_{CG} = 4.75m***

5.2.2 Elevator deflection effects on C_L, C_D, C_M, L/D at Mach=0 in clean wing configuration

Graphs below shows the effects of δ_e on each of the parameter.

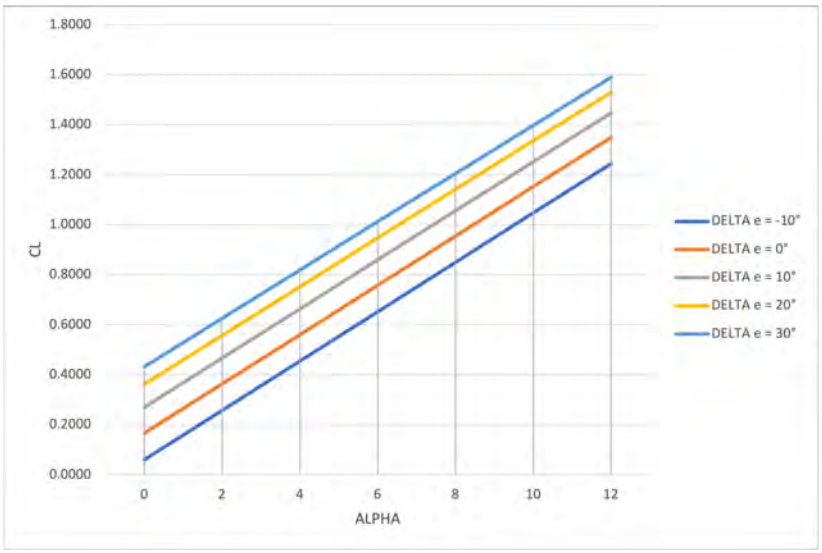

Figure 34 ***C_L with elevator deflection for L.H.T.P. with X_{CG} = 4.75m***

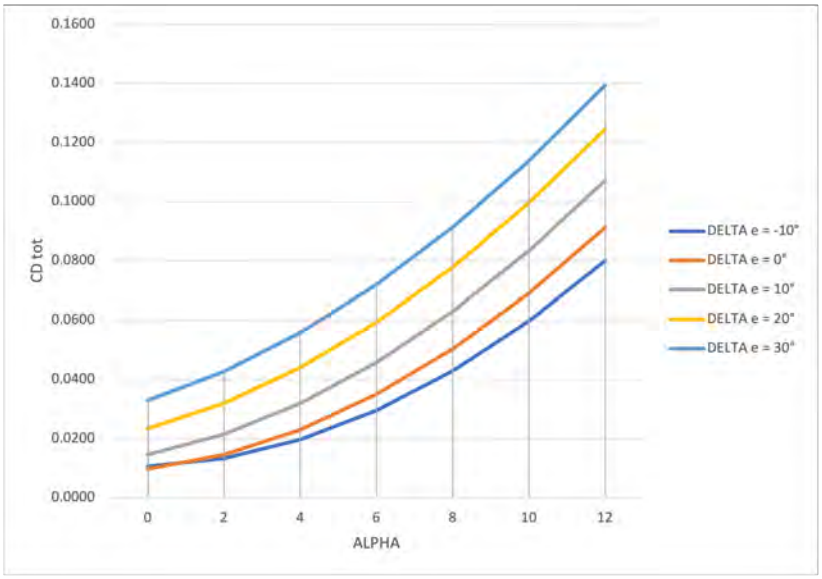

Figure 35 ***C_D with elevator deflection for L.H.T.P. with X_{CG} = 4.75m***

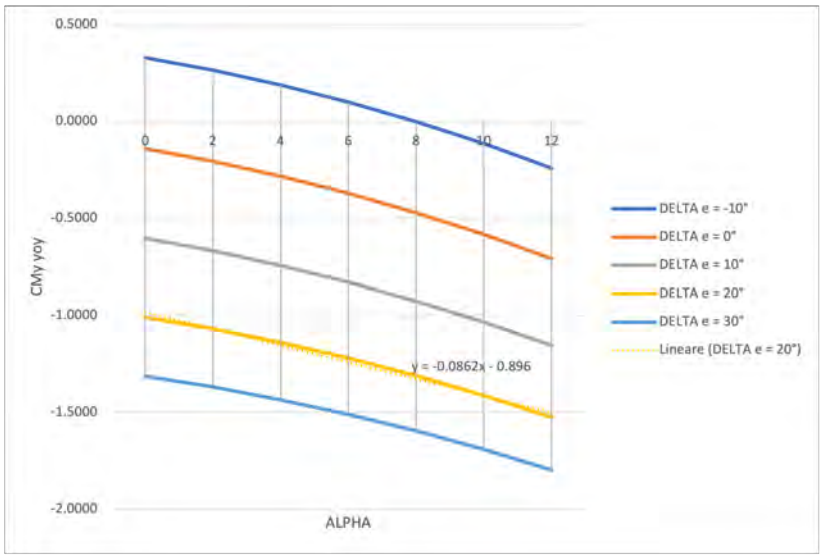

Figure 36 ***C_{My} with elevator deflection for L.H.T.P. with X_{CG} = 4.75m***

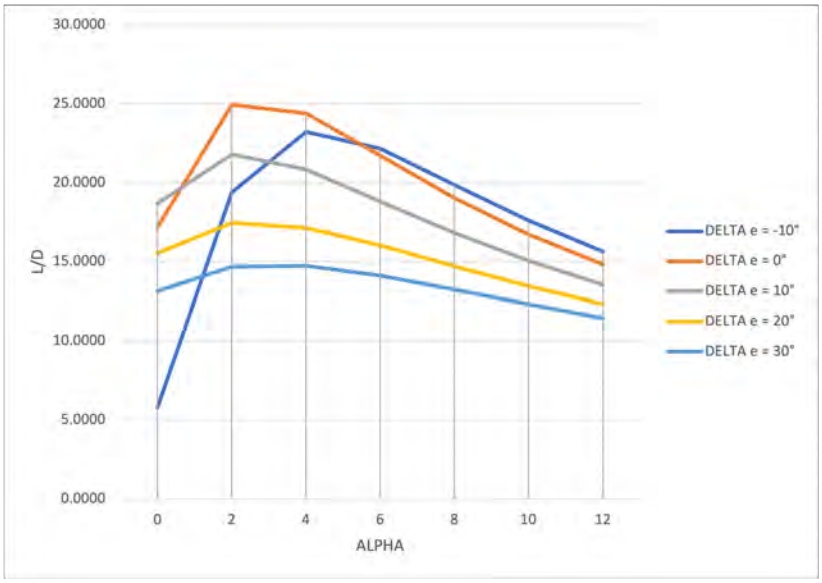

Figure 37 ***L\D with elevator deflection for L.H.T.P. with X_{CG} = 4.75m***

5.2.3 Derivatives

δf	*CMα*	*CM0*
0	-0.047	-0.112
10	-0.051	-0.040
20	-0.055	0.038
30	-0.059	0.112

δe	*CMy_tot*	*CMα*	*CM0*	*CMδ*
-10	0.328	-0.047	0.359	-0.047
0	-0.141	-0.047	-0.112	n.a.
10	-0.605	-0.046	-0.577	-0.047
20	-1.009	-0.043	-0.982	-0.044
30	-1.314	-0.040	-1.288	-0.039

Table 2 ***Stability and control derivatives (in deg^{-1}) for L.H.T.P. configuration with X_{CG} = 4.75m***

5.2.4 Results and possible solutions

Lowering the horizontal tail plane brings us almost the same results in terms of the effect of flap deflection, just as we have the same results for the effect of elevator deflection for the coefficients studied.

The same effect encountered in the previous case also occurs in the C_{My} curves of the case of horizontal tail panel placed in the safety zone dictated by the "Ramer: Aircraft design. A conceptual Approach" [6], figure 11.

An error on the CG position is assumed.

5.3 Effect of CG position on Aerodynamic Momentum Coefficient

Given the results of previous analysis a parametric study of CG position on Aerodynamic Momentum Coefficient (C_{My}) is performed. The figures below show the effects of CG position on C_{My} as angle of attack changes (α) and for two different flap deflections (δ_f =0°, δ_f = 20°).

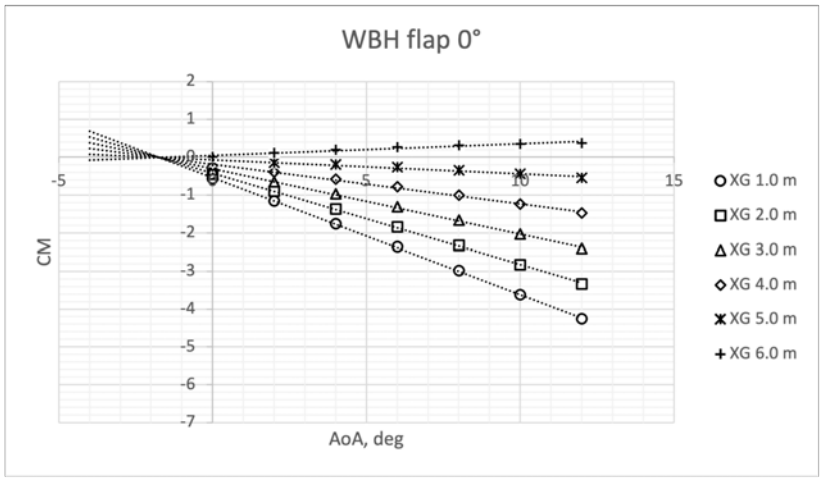

Figure 38 ***WBH effect of CG position on C_{My} with δ_f = 0°.***

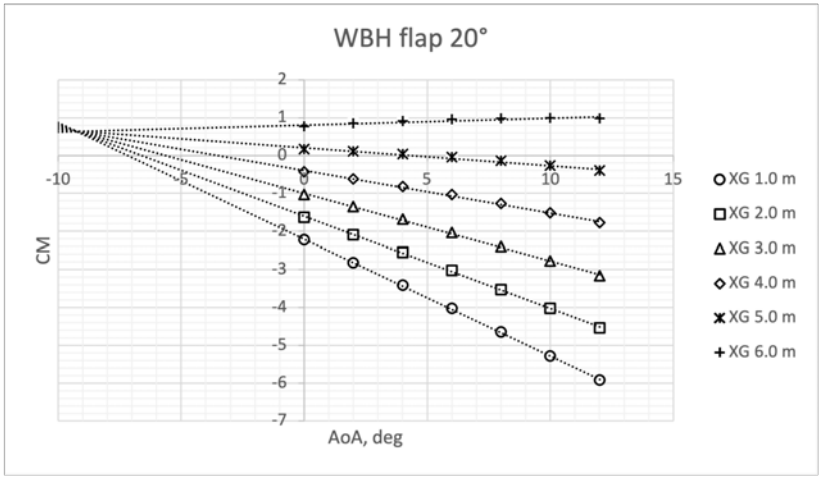

Figure 39 ***WBH effect of CG position on C_{My} with δ_f = 20°.***

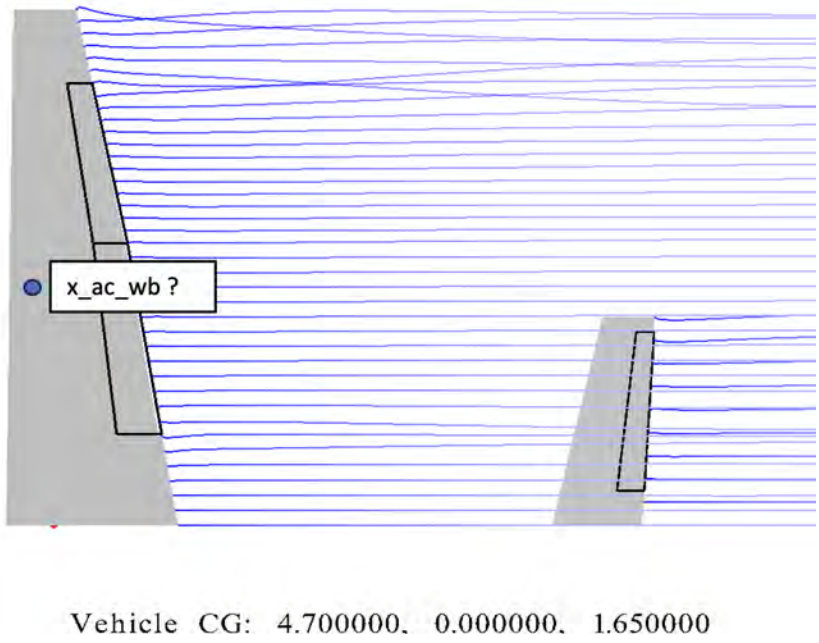

Figure 40 ***Position of initial CG with respect to X_{ac}. Red dot is CG, Blue dot is the supposed $x_{ac,WB}$.***

As result of the analysis performed a *CG position between 3.0m and 4.0m is suggested* since as the flap deflection increases (from 0° to 20°) the C_{My} curve becomes more negative (i.e., the WBH flap 0° X_{CG} = 3.0 m curve of figure 12 has greater values than the corresponding WBH flap 20° X_{CG} = 3.0 m curve of figure 13). An X_{CG} between 1.0 m and 3.0 m would also comply with this observation, but on its part a center of gravity in this range would exhibit values of the aerodynamic moment coefficient that are too negative.

With respect to these analyses the CG is placed in X_{CG} = 3.7 m, Y_{CG} = 0 m, Z_{CG} = 0.5 m.

5.3.1 Analysis of High Horizontal tail plane configuration with X_{CG} = 3.7 m, Z_{CG} = 0.5 m

Tables and figures below show the results in terms of aerodynamic pitching moment coefficient (C_{My}) of the analysis performed on T-tail configuration of Electra concept using a X_{CG} = 3.7 m.

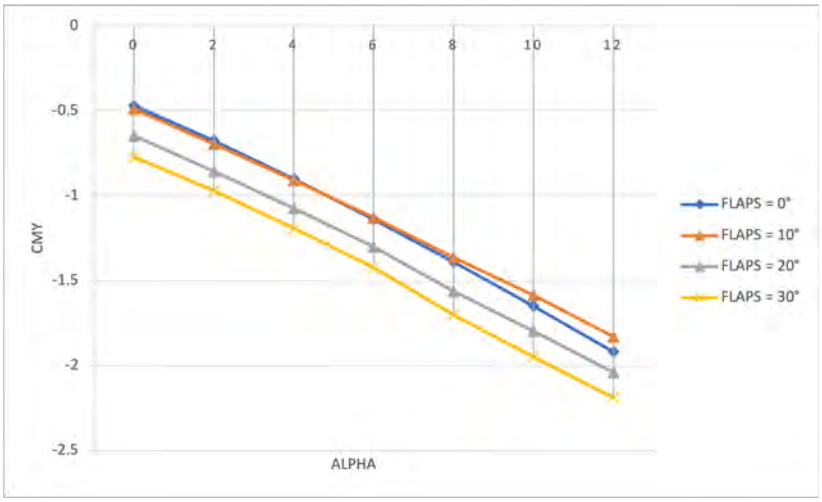

Figure 41 ***C_{My} with flaps deflection for H.H.T.P. with X_{CG} = 3.7 m***

Stability and control derivatives are calculated with respect to δ_f ranging from 0° up to 30° and δ_e ranging from -10° up to 30°.

δf	*CMα*	*CM0*
0	-0.121	-0.437
10	-0.112	-0.473
20	-0.117	-0.624
30	-0.120	-0.737

δe	*CMy_tot*	*CMα*	*CM0*	*CMδ*
-10	0.28292	-0.105	0.264	-0.070
0	-0.263417	-0.121	-0.437	n.a.
10	-0.80362	-0.105	-0.823	-0.039
20	-1.274463	-0.103	-1.283	-0.042
30	-1.6305822	-0.100	-1.627	-0.040

Table 3 ***Stability and control derivatives (in deg^{-1}) for H.H.T.P. configuration with X_{CG} = 3.7 m***

5.3.2 Analysis of Low Horizontal tail configuration with X_{CG} = 3.7 m, Z_{CG} = 0.5 m

Tables and figures below show the results in terms of aerodynamic pitching moment coefficient (C_{My}) of the analysis performed on low horizontal tailplane configuration of Electra concept using a X_{CG} = 3.7 m.

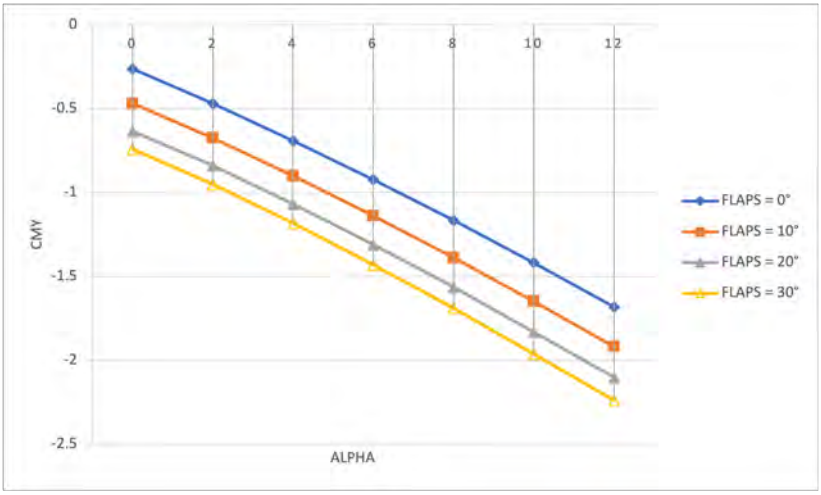

Figure 42 ***C_{My} with flaps deflection for L.H.T.P. with X_{CG} = 3.7 m***

Stability and control derivatives are calculated with respect to δ_f ranging from 0° up to 30° and δ_e ranging from -10° up to 30°.

δf	*CMα*	*CM0*
0	-0.118	-0.235
10	-0.121	-0.437
20	-0.123	-0.599
30	-0.125	-0.705

δe	*CMy_tot*	*CMα*	*CM0*	*CMδ*
-10	0.283	-0.119	0.313	-0.055
0	-0.263	-0.118	-0.235	n.a.
10	-0.804	-0.116	-0.777	-0.054
20	-1.274	-0.113	-1.250	-0.051
30	-1.631	-0.110	-1.607	-0.046

Table 4 ***Stability and control derivatives (in deg^{-1}) for L.H.T.P. configuration with X_{CG} = 3.7 m***

5.4 Propulsive effects on aerodynamic and stability of Electra's aircraft concept

Electra's eSTOL features 8 thrusters, 4 per wing, that aim to exploit DEP features such as "blown-lift" (as discussed in Chapter 2). The concept presents two different sizes of electric propellers: one has 1.302 m diameter and the other has 0.98 m diameter. Specifically, Electra uses the *REB50* (with 50 kW maximum power) and *RET60* (with 35 kW maximum power) motors [11]. Given the reference of "Mgm Compro" [12] and information about their electric motors that they supply to Electra through their partnership, it was possible to calculate the maximum takeoff thrust.

To study their effects on aerodynamics and stability the propellers are treat as actuator disks. Effects are studied in clean wing configuration and evaluated in three configurations of thrust:

- CRUISE [referred as *"prop-on cruise"*], it corresponds to point of max efficiency "E" on the drag polar curve, hence $C_D = 2C_{D0}$. Electra declared [7] $V_{\text{cruise}} = 200\ \text{mph} = 89.4\ \text{m/s}$ as cruise speed. An assumption about altitude has been made.

- MAX CLIMB [referred as *"prop-on climb"*], it corresponds to point "P" on the drag polar curve, hence $C_D = 4C_{D0}$. Climb speed is assumed half of cruise speed. $V_{\text{climb}} = 100\ \text{mph} = 44{,}7\ \text{m/s}$.

- TAKE-OFF [referred as *"prop-on take-off"*], it corresponds to a condition of maximum engine power. A take-off speed of $V_{\text{take-off}} = 80\ \text{mph} = 35\ \text{m/s}$ is considered.

An altitude of 10000 ft (3048 m) is supposed for both cruise and climb condition ($\rho =\backslash 0.9091\ \frac{\text{kg}}{\text{m}^3}$), while take-off condition is computer al sea level ($\rho = 1.225\ \frac{kg}{m^3}$.).

C_{D0} is computed using "Parasite Drag" tool of OpenVSP.

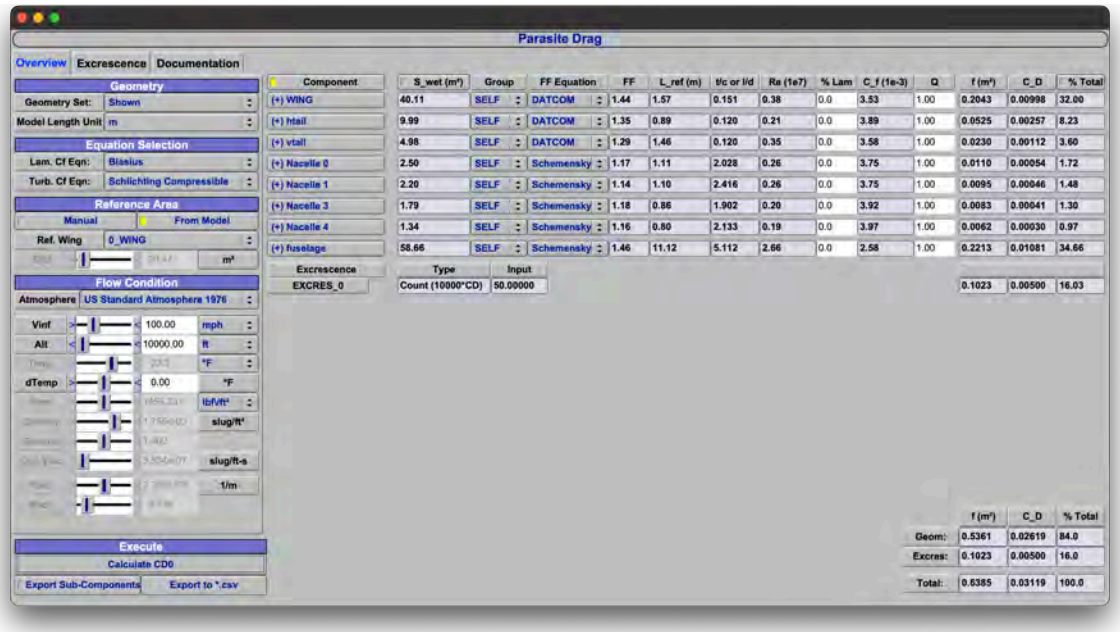

Figure 43 ***Parasite Drag panel in OPENVSP and parameters of climb analysis.***

Reference Area is the wing area of 20.47 m. DATCOM and Schemensky DATCOM RAND equations are set to compute the form factor FF. Q is a parameter representing the interference of each component (1.00 denotes no interference). Excrescence of 50 Drag Count is added to take into account possible protuberances and outgrowths (antennas, pitot tubes, etc.).

Max climb configuration presents $C_{D0} = 0.0312;\ C_D = 4C_{D0} = 0.1248$, while cruise condition has $C_{D0} = 0.0285;\ C_D = 2C_{D0} = 0.0570$.

To run the analyses with the electric propeller on, after activating the "actuator disk" toggle in the "advanced" panel, VSPAERO requires for each of the 8 propellers: RPM, C_T (Thrust coefficient), C_P (shaft power coefficient). The last one was calculated assuming a propeller efficiency $\eta = 0.8$. To compute these parameters in cruise and climb, a level flight condition (Thrust = Drag) is assumed.

$$T = D;\ \ D = \frac{1}{2}\rho_\infty V_\infty^2 S C_D$$

For the take-off condition, static thrust ($V = 0$) was calculated with the following equation:

$$T_0 = \sqrt[3]{P^2\left(\eta^2\pi\frac{D^2}{2}\rho_\infty\right)}$$

C_T and C_P are calculated as equations below show, where $n = \frac{RPM}{60}$ and D is the propeller diameter.

$$C_T = \frac{T}{\rho_\infty n^2 D^3}$$

$$C_P = \frac{P}{\rho_\infty n^3 D^5}$$

5.4.1 Cruise condition

For cruise condition, corresponding to "*E*" point of the drag polar, the total thrust computed is equal to 4241 N. An equal thrust profile is assumed for all the propellers, resulting in 530,14 N for each one. Total shaft power is equal to 30.336 kW, resulting in approximately 37.92 kW on each propeller.

Bigger propeller present RPM = 3000, C_T = 0.1057, C_P = 0.1393, while for smaller propeller RPM = 3500 , C_T = 0.1821, C_P = 0.3632.

5.4.2 Max climb condition

Climb condition corresponds to "*P*" point on drag polar, thus C_D is computed as four times the parasite drag. The total thrust required is equal to 5211 N, that correspond to 651.4 N for each propeller. Total shaft power is equal to 436420 W, resulting in 54553 W on each electric generator.

Bigger propeller present RPM = 3000, C_T = 0.1299, C_P = 0.1283, while for smaller propeller RPM = 3500 , C_T = 0.2237, C_P = 0.3344.

5.4.3 Take-off condition

The take-off condition is studied using static thrust as a parameter in the C_T coefficient. The powers used to compute T_0 correspond to the maximum powers of the REB50 and RET60 engines of 50 kW and 35 kW, respectively. Also, in this configuration 3000 RPM is

assumed, which leads us to have for the larger engines a $C_T = 0.2938$ and a $C_P = 0.1069$. Smaller engines have $C_T = 0.4494$ and $C_P = 0.3098$.

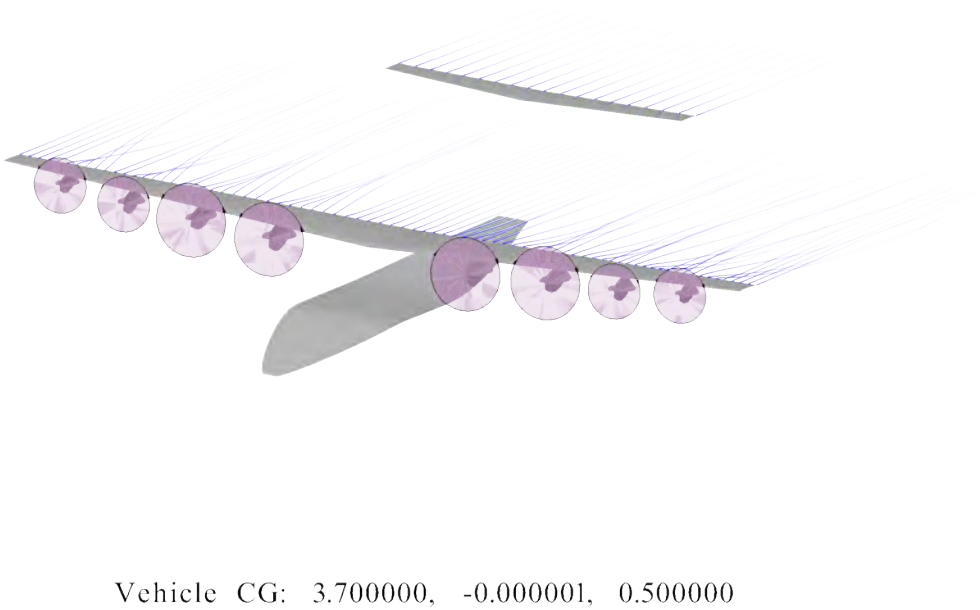

Figure 44 ***Visualization of wake due to propeller effects.***

5.4.4 Effects on C_L, C_D, C_{My}.

Figures below show the comparison of effects of DEP in cruise configuration (prop-on cruise), climb (prop-on climb) and take-off (prop-on take-off) configuration against the propulsors off case (prop-off).

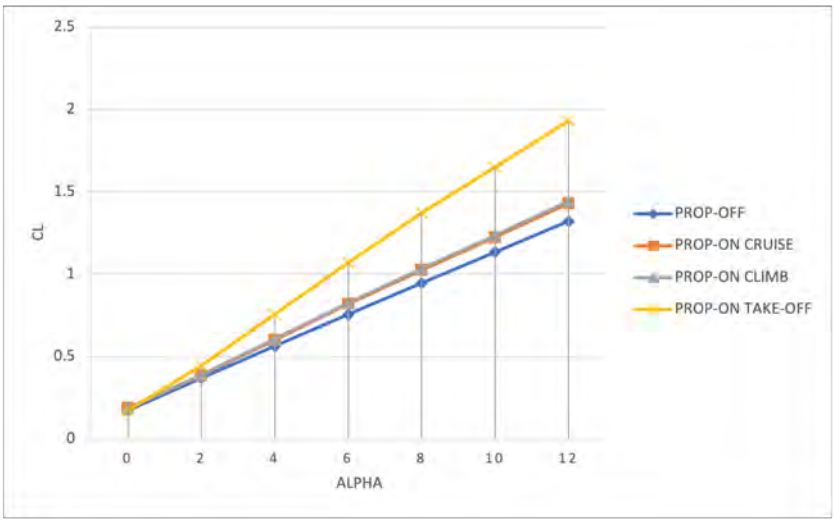

Figure 45 ***C_L vs α, comparison between prop-on cruise, prop-on climb, prop-on take-off and prop-off configuration.***

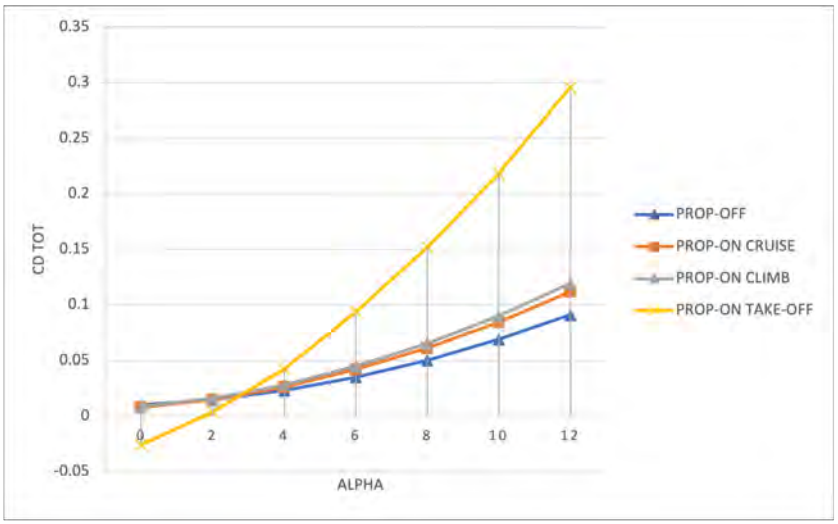

Figure 46 ***C_D vs α, comparison between prop-on cruise, prop-on climb, prop-on take-off and prop-off configuration.***

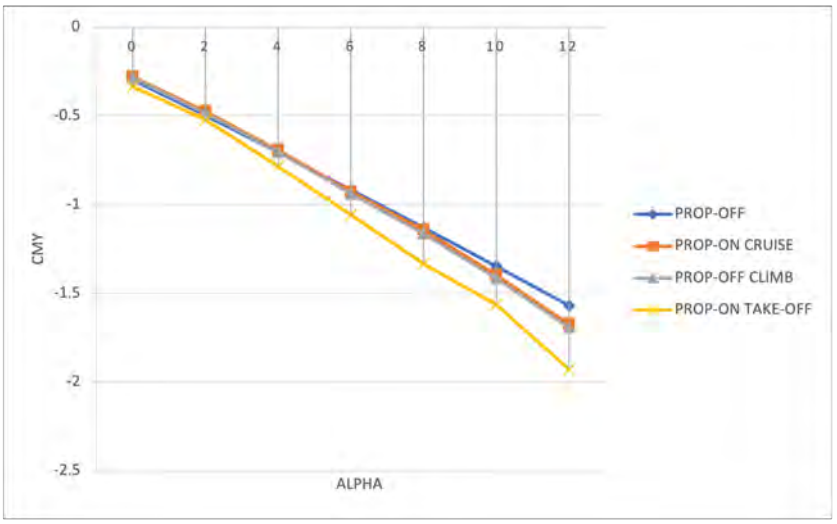

Figure 47 ***C_{My} vs α, comparison between prop-on cruise, prop-on climb, prop-on take-off and prop-off configuration.***

The cruise and climb cases both have similar and slightly higher C_L and C_D coefficients than the "prop-off" case, as well as a slightly more negative C_{My} for high angles of attack (10° and 12°). Particular, however, is the condition of maximum take-off thrust, in which in addition to having a significant effect on lift by means of a higher C_L (due to the blowing effect of the propellers on the wing) and on stability by means of a significantly steeper C_{My} curve, provides a negative drag for $\alpha \leq 2°$. This is due to the aerodynamic load induced to the wing by the distributed thrust, while the additional parasite drag due to the local blowing is not correctly calculated by VSPAERO. Clearly, the drag and its aerodynamic coefficient cannot be negative.

6 Conclusions

To conclude the thesis, the detailed analysis conducted on the Electra eSTOL aircraft concept has revealed a significant challenge related to the static stability induced by the effects on the aerodynamic coefficients. However, through thorough examination, solutions have been identified that can effectively mitigate this issue, enhancing the overall stability of the aircraft.

The proposed adjustment of placing the center of gravity between 3 and 4 meters from the fuselage nose, regardless of the investigated positions of the horizontal tailplane, emerges as a viable solution to address the enhance the aircraft longitudinal stability and control and ensure safe behavior throughout all flight phases.

The issue concerning the load distribution during take-off conditions has also been addressed by identifying a limit in VSPAERO calculation of parasite drag. Introducing corrections in the drag calculations should help ensure that drag does not become negative during flight phases, ensuring a more accurate and realistic simulation.

In summary, the proposed solutions will provide a solid foundation for further developments and refinements of the Electra's eSTOL concept, overcoming challenges identified during this stability analysis.

References

[1] "Design and Performance of the NASA SCEPTOR Distributed Electric Propulsion Flight Demonstrator"

[2] "Comparison of Aero-Propulsive Performance Predictions for Distributed Propulsion Configurations"

[3] Sean Clarke: "SCEPTOR Power System Design: Experimental Electric Propulsion System Design and Qualification for Crewed Flight Testing" "A Review of Distributed Electric Propulsion Concepts for Air Vehicle Technology"

[4] Jason A. Lechniak and Others: "LEAPTech/HEIST Experiment Test and Evaluation Summary"

[5] Università degli Studi di Napoli Federico II. Disponibile al sito: http://www.unina.it/home (accesso effettuato il 23/07/2022)

[6] OpenVSP. Available at www.openvsp.org

[7] Electra Aero. Available at www.electra.aero

[8] JPAD software. Available at https://www.smartup-engineering.com/jpad

[9] Cessna Caravan. Available at www.cessna.txtav.com/en/turboprop/caravan#_model-specs

[10] Daniel P. Raymer: "Aircraft Design: A conceptual Approach"

[11] Mgm Compro, partnership with Electra available at www.mgm-compro.com/reference/electra-aero

[12] REB50 Electric motor and RET60 electric motor, available at www.mgm-compro.com/electric-motor/50-kw-electric-motor/ and www.mgm-compro.com/electric-motor/35-kw-electric-motor/